

POLITECNICO DI TORINO

Corso di Laurea Magistrale in Ingegneria  
Civile

Tesi di Laurea Magistrale

**Theory and application of the Wave  
Finite Element method to the  
dynamic analysis of multi-supported  
bridges**



**Relatrice:**

Prof.ssa Cecilia Surace

**Correlatori:**

Prof.ssa Maria Giuseppina Limongelli

Prof. Denis Duhamel

Dott. Tien Hoang

Prof. Gilles Foret

**Candidato:**

Gabriele Paratore

Aprile 2019

*Vorrei ringraziare in primis la professoressa Surace per avermi dato la possibilità di trascorrere questa esperienza di studio all'École des Ponts ParisTech.*

*Un grazie speciale va alla simpaticissima professoressa Limongelli che mi ha seguito ed incoraggiato durante tutto il percorso dedicandomi gran parte del suo tempo.*

*Ringrazio il team di cui ho fatto parte all'interno laboratorio Navier composto dal prof. D.Duhamel, dal prof. G. Foret e dal dott. T. Hoang.*

*Vorrei particolarmente ringraziare Tien il quale è stato la mia guida principale durante tutto il lavoro di tesi.*

*Grazie anche a Marie-Françoise, per la sua disponibilità e la sua simpatia.*

*Grazie agli amici di Parigi con cui ho passato bellissimi momenti e a tutti coloro i quali mi sono stati a fianco durante questo lungo percorso.*

*Infine ringrazio la mia famiglia perchè senza di loro non avrei mai potuto raggiungere questo traguardo.*

*J'aimerais tout d'abord remercier la professeure Surace qui m'a permis de réaliser cette expérience d'étude à l'Ecole des Ponts ParisTech.*

*Je voudrais remercier aussi la professeure Limongelli, qui a été très disponible et qui m'a suivi et encouragé pendant toute la durée de mon projet, en me dedicant une grande partie de son temps.*

*Je remercie l'équipe du laboratoire Navier dont j'ai fait partie:*

*le prof D. Duhamel, le prof. G. Foret et le dr. T. Hoang.*

*Un remerciement particulier va à Tien, qui a été mon principal guide tout au long du projet.*

*Merci également à Marie-Françoise pour sa disponibilité et sa sympathie.*

*Merci aux amis parisiens, car j'ai passé des très beaux moments avec eux, et à tous ce qui m'ont accompagné dans mon long chemin.*

*Enfin, merci à ma famille, car c'est grâce à eux que j'ai pu atteindre ce grand objectif.*

## Abstract

The phenomenon of wave propagation in periodic structures is first introduced focusing the attention on the wave characteristics - e.g. propagation constants - which help to best understand the physic of the problem.

The *wave finite element* (WFE) method is then discussed and two different approaches of resolution are described: the *dynamic stiffness matrix* (DSM) approach and the *wave amplitude* (WA) approach.

The method is further extended to account for the presence of intermediate supports along the structure. This application of the WFE is a new development that represents the main core of the thesis. Several case studies are developed (1D beam, 2D beam, and a real bridge) using a Matlab script written on purposes. The results are compared with the conventional application of the finite element (FE) method. This allows to assess the solution and to highlight the low computational effort associated to the use of the WFE with respect to the more traditional FE.

# Contents

<b>Introduction</b>	<b>3</b>
<b>1 Basic Framework</b>	<b>5</b>
1.1 Periodic structures . . . . .	5
1.2 Wave propagation in periodic structures . . . . .	7
1.2.1 Bloch's Theorem . . . . .	8
1.2.2 Wave number . . . . .	8
1.2.3 Propagation constant . . . . .	9
<b>2 Wave finite element method</b>	<b>11</b>
2.1 Basis of WFE method . . . . .	12
2.2 Wave analysis . . . . .	16
2.2.1 Property of wave vectors . . . . .	17
2.2.2 Solution of the eigenvalue problem . . . . .	18
2.2.3 Physical meaning of wave-modes . . . . .	20
2.3 Approaches of the WFE method and analysis of a complete structure . . . . .	21
2.3.1 Wave Amplitude (WA) approach . . . . .	21
2.3.2 Dynamic stiffness matrix (DSM) approach . . . . .	27
2.4 Application of the WA approach . . . . .	27
<b>3 New application of the WFEM</b>	<b>29</b>
3.1 Derivation of the intermediate reactions . . . . .	30
3.2 Boundary conditions . . . . .	32
3.2.1 Index matrix $\mathbf{L}$ . . . . .	34
3.2.2 Vector of boundary conditions $\mathbf{B}$ . . . . .	37
3.3 Solution of the problem . . . . .	37
3.3.1 Definition of the linear system . . . . .	38
3.3.2 Solution of the linear system . . . . .	41

<b>4 Applications</b>	<b>43</b>
4.1 1D Beam . . . . .	44
4.1.1 Problem statement . . . . .	44
4.1.2 Description of the substructure . . . . .	44
4.1.3 Results and comments . . . . .	45
4.2 2D Beam . . . . .	46
4.2.1 Problem statement . . . . .	46
4.2.2 Description of the substructure . . . . .	47
4.2.3 Results and comments . . . . .	48
4.3 Multi-supported bridge . . . . .	49
4.3.1 Description of the structure . . . . .	49
4.3.2 Description of the substructure . . . . .	50
4.3.3 Results and comments . . . . .	51
4.4 General comments . . . . .	52
<b>Conclusions</b>	<b>53</b>
<b>Annex A</b>	<b>54</b>
<b>Annex B</b>	<b>55</b>
<b>Bibliography</b>	<b>56</b>

# Introduction

The Wave Finite Element (WFE) is a powerful numerical method that allows to drastically reduce the number of degrees of freedom of a structural model providing a great advantage in terms of computational time. This method have been developed for periodic structures where the geometry repeats itself in a certain direction, and is based on wave propagation. The objective is to compute the wave modes which constitute a base that, similarly to the eigen modes often used in the dynamic analysis, can be used to decompose the structural response in terms of forces and displacements at the considered degrees of freedom. The wave modes are characteristics of the elementary periodic element therefore they can be computed by solving an eigenvalues problem consistently formulated for this element. According to the approach proposed by Duhamel et al. [1] the periodic element can be modelled using the conventional finite element method to retrieve its mass, stiffness and damping matrices. In this approach, these matrices are then used to obtain the dynamic stiffness of the cell in the frequency domain and the theory of periodic structure is used to build the dynamic stiffness matrix of the whole structure. Once the wave base has been determined for the period of the structure and the dynamic problem formulated in terms of this base, the solution of the dynamic equation can be carried out by imposing the boundary conditions. This approach has been followed in Hoang et al. [2] that proposed the wave approach, based on the computation of the dynamic response as the sum of different wave contributions generated by the forces acting on the structure. In previous studies [2, 3], the WFE has been applied considering constrains applied only at the ends of the structure or included inside the periodic element, as is the case of railway tracks. The objective of this thesis has been to extend the application of the WFE to the study of the dynamic response of multi-supported periodic structures. The cooperation with D. Duhamel and G. Foret and T. Hoang, at Laboratoire Navier, École des Ponts ParisTech where I spent an exchange period as part of their team, allowed me to master the method and to extended it, including the possibility to account for different types of boundary conditions. The extension

proposed in this thesis allows to analyse structures, such as bridges, whose supports may be of different types and are not necessarily equally spaced. The thesis is structured in four chapters. The first is dedicated to the introduction of the problem starting from the type of structures considered in the study and from a more detailed explanation from a physical point of view. The second chapter deals with the WFE and the approaches of resolution. In the last section of the chapter the example of a simply supported structure is developed and used to introduce the fundamental chapter of the thesis. The third chapter contains the original part of this thesis dealing with the analytical formulation of the WFE of a periodic structure with multiple intermediate supports. Finally, in the fourth chapter the numerical results obtained using a Matlab script, implemented on purpose, will be presented with reference to a number of case studies.

# Chapter 1

## Basic Framework

This chapter introduces the basic concept of wave propagation in periodic structures which can be seen as wave-guides. The first section deals with the definition and examples of one-dimensional and two-dimensional periodic structures.

The second section will introduce the concept of wave propagation in periodic structures which represent the theoretical fundamentals of the WFE method. Firstly the Bloch's Theorem will be presented, and then the propagation constants will be commented.

### 1.1 Periodic structures

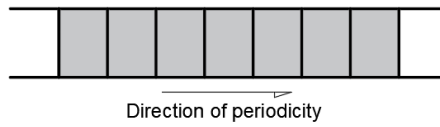
A *periodic system* consists of a number of identical elements, in terms of geometric shape, physical properties, boundary conditions, and connections with other substructures, coupled together to form the whole system.

The atomic lattices of pure crystals constitute perfect periodic structures but these are lumped parameter systems with discrete masses (the atoms) interconnected by the inter-atomic elastic forces. In structural engineering the mass and elasticity of structural members are continuous and constitute periodic structures when arranged in regular arrays.

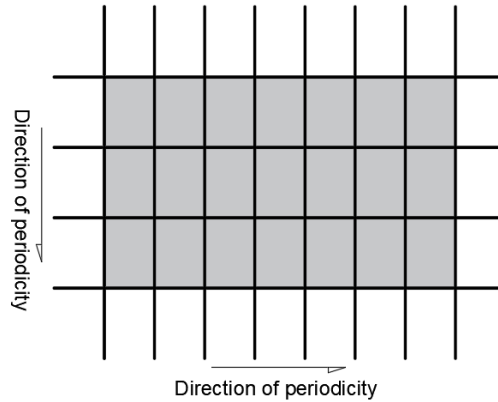
A periodic system can be:

- *one-dimensional*: the elements are connected end-to-end, or side-by-side through multiple coupling coordinate between them.
- *two-dimensional*: the elements are assembled both end-to-end and side-by-side where multiple coupling between adjacent elements is allowed on all sides.

In Figure (1.1) the two types of systems are represented.



(a) *One-dimensional periodic system.*



(b) *Two-dimensional periodic system.*

Figure 1.1: Schematic diagram of periodic systems.

In the engineering field, several structures can be considered as periodic system. Examples of such a system are: multi-storey buildings having a uniform structure and identical storeys, aeroplane fuselage structure consisting of a uniform shell reinforcement at regular intervals by an orthogonal set of identical stiffeners, multi-span bridges, multi-blade turbines and rotary compressors, chemical pipelines, stiffened plates and shells in aerospace and ship structures, space station structures and layered composite structures.

In the design of these structures, account must be taken of the vibration levels likely to be caused by time dependent forces, pressure or motions to be encountered in service life. The associated levels of vibration and shock response must be predictable in order to design the structure with a minimum probability of catastrophic damage or malfunction in service.

A periodic system can be seen as a wave-guide, namely a structure that guides waves. The periodicity property allows a great simplification in the analysis of the vibrations. It is almost unnecessary to study the principal modes, as the periodicity has vibration characteristic that are best understood in terms of propagating and non-propagating waves. In the next section the principal concepts of wave propagation in periodic structure will be introduced.

## 1.2 Wave propagation in periodic structures

The first studies of *wave propagation in periodic structures* go back three hundred years ago affirms Brillouin in his work[5]. In the attempt to derive a formula for the velocity of sound, Isaac Newton worked on a one-dimensional lattice of point masses (at that time a continuous structure represented an insoluble problem). In the following years, the studies were improved thanks to more powerful mathematics tools. Physicists and electrical engineers developed this subject in relation to crystals, optics, electrical transmission lines, etc. It is only recently that wave motion in engineering periodic structures (consisting of beams, plates, etc.) has been investigated.

The periodic structure presents a filter characteristic, which is also called the *band diagram*, and is the most important wave propagation characteristics in periodic structures. The associated *dispersion diagram*, represents the change in frequency with the *wave number*. In Figure (1.2) is shown an example. It is also called dispersion relation describing the nature of free wave propagation in an elastic medium.

Is known that when a dynamic excitation is applied to a generic structure, it generates elastic waves that propagate depending on the frequency of vibration. Indeed, not all the waves propagate since interference leads to the formation of *band gaps*<sup>1</sup> that prevent waves with certain frequencies travelling through the structure [6].

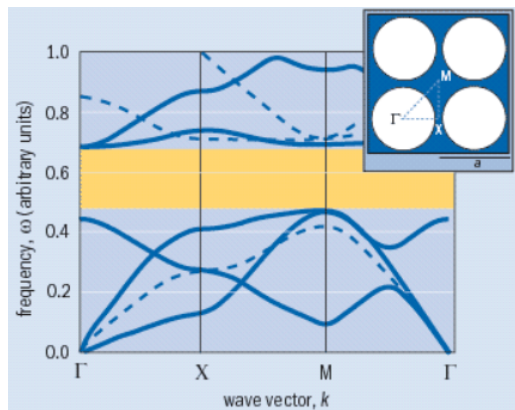


Figure 1.2: Example of dispersion diagram.

The existence of band gaps in periodic structure, can lead to interesting application such as vibration isolation or wave guiding. Studying the property of the structure, is possible to predict which wave will propagate along

---

<sup>1</sup>A *band gap* is a range of wavelength or frequency within which waves cannot propagate through the structure.

the structure. The number of propagating waves depends on the frequency of vibration and generally their number increase with the increasing of the perturbation's frequency.

### 1.2.1 Bloch's Theorem

The wave propagation in periodic structure obeys to the Bloch's theorem. In solid state-physics, this theorem represent the analogue result of Floquet's theorem [7]. The Bloch's wave theorem is expressed by the following expression[8]:

$$\mathbf{u}(\mathbf{x}, t) = \bar{\mathbf{u}}(\mathbf{x}) e^{i(\mathbf{k}\mathbf{x} - \omega t)} \quad (1.1)$$

where  $\mathbf{u}$  is the displacement,  $\bar{\mathbf{u}}$  is a periodic wave function depending only on the position  $\mathbf{x}$ ,  $\mathbf{k}$  is the wave vector,  $\omega$  is the forcing frequency and  $t$  is the time.

Equation (1.1) states that the displacement at one end of a periodic element is a factor of  $e^{-i\mathbf{k}\mathbf{x}}$  times the displacement of the other end.

### 1.2.2 Wave number

The *wave vector*  $\mathbf{k}$  is the generalization of the *wave number*  $k$  for multidimensional systems. It describes how the wave propagates from one cell to the adjacent. It can be a complex number and both the real and imaginary parts have a specific physical meaning:

- The *Real part* represent the *propagation constant* and characterises the phase shift of the wave.
- The *Imaginary part* is the *attenuation constant* and describes the *attenuation* of the wave along the periodic element.

When damping is present,  $\mathbf{k}$  is always complex because energy is dissipated and this causes always an attenuation of the wave.

The study of the relationship between the wave number  $k$  and the frequency  $\omega$  provides the band structure expressed by the dispersion curve. In this way the location and width of band gaps can be found.

### 1.2.3 Propagation constant

Consider a general element of an infinite period structure represented in Figure (1.3).

The Bloch theorem for wave propagation in one-dimensional periodic structures can be written in the following way:

$$\begin{bmatrix} \mathbf{q}_R \\ -\mathbf{F}_R \end{bmatrix} = e^\beta \begin{bmatrix} \mathbf{q}_L \\ \mathbf{F}_L \end{bmatrix} \quad (1.2)$$

where the subscripts "L" and "R" stand for left and right. The exponent  $\beta$  is the *propagation constant* and is related to the *wave number*  $k$  by:

$$\beta = -ikL \quad (1.3)$$

Where  $L$  is the length of the periodic element.

From equation (1.3) is possible to observe that also the propagation constant  $\beta$  is a complex number and that the meaning of the real and imaginary part are changed with respect to the wave number.

The propagation constants come in pair of positive and negative values  $\pm\beta$  for each given frequency  $\omega$ .

The computation of the propagation constants thus provides the complex frequency band structures of the infinitive periodic system.

The two propagation constants in each pair represent essentially the same characteristic wave but travelling in opposite directions. In general, some of the propagation constants may be real, some purely imaginary, and some complex.

Physically, three regions on the frequency axis can be distinguished for each pair of propagation constants [9]:

- **Attenuation region.** The propagation constant is of the form  $\beta = Re(\beta) + in\pi$ , with  $n$  integer and  $|Re(\beta)| > 0$ . The wave is attenuated with the adjacent unit cells vibrating in phase or out of phase.

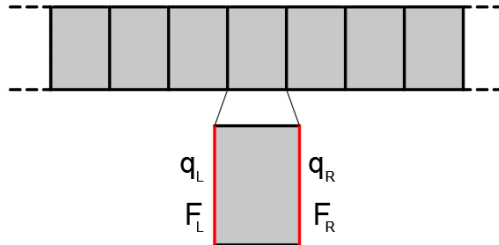


Figure 1.3: General substructure.

- **Propagation region.** The propagation constant is purely imaginary, i.e.,  $\beta = i \text{Im}(\beta)$  with  $2n\pi < |\text{Im}(\beta)| < (2n + 1)\pi$  and  $n$  integer. The wave is propagating without attenuation and with a phase change at each unit cell.
- **Complex region.** The propagation constant has the form  $\mu = \text{Re}(\beta) + i \text{Im}(\beta)$ , with  $|\text{Re}(\beta)| > 0$  and  $2n\pi < |\text{Im}(\beta)| < (2n + 1)\pi$ . The wave is propagating and attenuating along the system.

The propagation constant can be computed using the Transfer Matrix (TM) method. The *transfer matrix*  $\mathbf{S}$ , relates the displacements  $\mathbf{q}$  and forces  $\mathbf{F}$  on the two sides of the periodic element by the relationship:

$$\begin{bmatrix} \mathbf{q}_R \\ -\mathbf{F}_R \end{bmatrix} = \mathbf{S} \begin{bmatrix} \mathbf{q}_L \\ \mathbf{F}_L \end{bmatrix} \quad (1.4)$$

Substituting equation (1.2) in equation (1.4), we obtain an eigenvalue problem in the form:

$$\mathbf{S} \begin{bmatrix} \mathbf{q}_L \\ \mathbf{F}_L \end{bmatrix} = e^\beta \begin{bmatrix} \mathbf{q}_L \\ \mathbf{F}_L \end{bmatrix} \quad (1.5)$$

Hence, each eigenvalue of the matrix  $\mathbf{S}$  provide the propagation constant while the eigenvector, represent the wave shapes, namely the way in which the substructure deforms. The wave finite element method uses the FE model of the substructure to derive the transfer matrix  $\mathbf{S}$  as we'll see in the next chapter.

# Chapter 2

## Wave finite element method

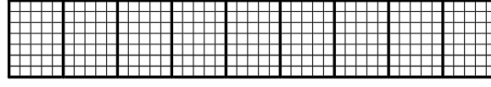
The wave finite element (WFE) method is a methods based on the wave propagation in periodic structures. This method allow to calculate the free and forced response of a periodic structure combining together the phenomenon of wave propagation in periodic structure and the Finite Element Method (FEM). Thanks to the special property of periodicity, the dynamic study of the entire structure can be reduced to that of the single periodic element (substructure) like the one represented in Figure (2.2). The remarkable feature of this approach is that it can be easily implemented on MATLAB<sup>®</sup>, and yields small computational time compared to dedicated FE Software.

For a periodic structure or wave-guide, is possible to obtain a transformation for the vector of *degrees of freedom* (DOF) and *nodal forces* on the left and right boundaries form the dynamic equation of one period. The eigenvectors of the transformation form a wave base which can be used to calculate the response by the the *dynamic stiffness matrix* (DSM) approach or the *wave amplitude* (WA) Approach.

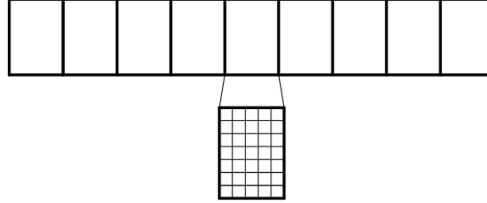
The first approach consists in deriving the DSM of the entire structure starting from the DSM of the general substructure while the second is based on the calculus of the wave amplitudes of the waves that travel in the structure. Only the latter approach will be discussed whether the DSM Approach will be only mentioned.

The methods presented is an extension of the classical WFE method [1, 4] and permit to consider the structure subjected to any type of loads [2].

In the fist section the transfer matrix will be derived starting from the FE analysis of a single substructure. The second section treats the wave analysis: the eigenvalue problem will be solved and the two approaches will be showed. Finally, an application of the WA approach is shown in order to introduce the next chapter.



(a) *Meshing the entire structure.*



(b) *Meshing only a section of the entire structure.*

Figure 2.1: Comparison between Wave Finite Element Method (WFEM) and Finite Element Method (FEM)

## 2.1 Basis of WFE method

Consider a generic infinite *one-dimensional* periodic structure composed by cells linked end-to-end, which are identical in terms of geometrical and mechanical properties. Each substructure is connected to the adjacent ones by the left and right bound. Using the FE method, the generic element is modelled and two types of nodes can be defined: *internal nodes* and *boundary nodes*. The boundary nodes are in turn divided into *left nodes* and *right nodes* with  $d$  *degrees of freedom* (DOFs) for each side.

The kinematic behaviour of the system is described by the column vector of nodal displacements  $\mathbf{q}$  which number of components is equal to the total number of DOFs of the substructure. On the other hand, the respective nodal forces are described by the column vector  $\mathbf{F}$ . Their relation is given by the discrete equation of motion:

$$\mathbf{M}\ddot{\mathbf{q}}(t) + \mathbf{C}\dot{\mathbf{q}}(t) + \mathbf{K}\mathbf{q}(t) = \mathbf{F}(t) \quad (2.1)$$

Where  $\mathbf{M}$ ,  $\mathbf{C}$  and  $\mathbf{K}$  are respectively the Mass, Damping and Stiffness Matrix and  $\ddot{\mathbf{q}}$  and  $\dot{\mathbf{q}}$  are the first and second derivative of the displacement vector with respect to the time.

Trough a Fourier Transform, equation (2.1) can be written in the frequency domain as follow (see Annex A):

$$(\mathbf{K} + i\omega\mathbf{C} - \omega^2\mathbf{M})\mathbf{q}(\omega) = \mathbf{F}(\omega) \quad (2.2)$$

or in a more compact form,

$$\mathbf{D}(\omega)\mathbf{q}(\omega) = \mathbf{F}(\omega) \quad (2.3)$$

where  $\mathbf{D}$  is the *dynamic stiffness matrix* (DSM), defined as:

$$\mathbf{D}(\omega) = \mathbf{K} + i\omega\mathbf{C} - \omega^2\mathbf{M} \quad (2.4)$$

The dynamic equation can be rewritten in the expanded form in order to separate the degrees of freedom into left (L), inner (I) and right (R) ones like highlighted in Figure (2.2).

$$\begin{bmatrix} \mathbf{D}_{LL} & \mathbf{D}_{LI} & \mathbf{D}_{LR} \\ \mathbf{D}_{IL} & \mathbf{D}_{II} & \mathbf{D}_{IR} \\ \mathbf{D}_{RL} & \mathbf{D}_{RI} & \mathbf{D}_{RR} \end{bmatrix} \begin{bmatrix} \mathbf{q}_L \\ \mathbf{q}_I \\ \mathbf{q}_R \end{bmatrix} = \begin{bmatrix} \mathbf{F}_L \\ \mathbf{F}_I \\ \mathbf{F}_R \end{bmatrix} \quad (2.5)$$

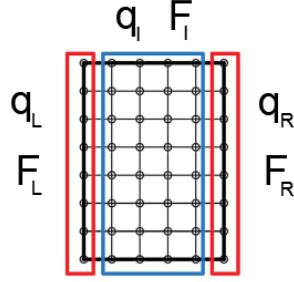


Figure 2.2: Left, inner and right nodes of a general substructure.

Free wave motion occurs when  $\mathbf{F}_I = 0$ . The exterior nodal forces  $\mathbf{F}_L$  and  $\mathbf{F}_R$  are not zero since they are the means whereby wave motion is transmitted from one element to the other.

Writing the inner degrees of freedom  $\mathbf{q}_I$  in function of the boundary DOF  $\mathbf{q}_R$  and  $\mathbf{q}_L$ , we can reduce the inner nodes in order to obtain a condensed form of the dynamic stiffness matrix.

From the first row of equation (2.5):

$$\mathbf{q}_I = \mathbf{D}_{II}^{-1} [\mathbf{F}_I - \mathbf{D}_{IL}\mathbf{q}_L - \mathbf{D}_{IR}\mathbf{q}_R] \quad (2.6)$$

Placing this equation in the first and last row of equation (2.5):

$$\begin{aligned} \mathbf{D}_{LL}\mathbf{q}_L + \mathbf{D}_{LI}\mathbf{D}_{II}^{-1} [\mathbf{F}_I - \mathbf{D}_{IL}\mathbf{q}_L - \mathbf{D}_{IR}\mathbf{q}_R] + \mathbf{D}_{LR}\mathbf{q}_R &= \mathbf{F}_L \\ \mathbf{D}_{RL}\mathbf{q}_L + \mathbf{D}_{RI}\mathbf{D}_{II}^{-1} [\mathbf{F}_I - \mathbf{D}_{IL}\mathbf{q}_L - \mathbf{D}_{IR}\mathbf{q}_R] + \mathbf{D}_{RR}\mathbf{q}_R &= \mathbf{F}_R \end{aligned}$$

Finally, gathering the terms with respect to the internal forces, the nodal displacement and the nodal forces of the boundaries:

$$\begin{aligned}\mathbf{D}_{LI}\mathbf{D}_{II}^{-1}\mathbf{F}_I + (\mathbf{D}_{LL} + \mathbf{D}_{LI}\mathbf{D}_{II}^{-1}\mathbf{D}_{IL})\mathbf{q}_L + (\mathbf{D}_{LR} + \mathbf{D}_{LI}\mathbf{D}_{II}^{-1}\mathbf{D}_{IR})\mathbf{q}_R &= \mathbf{F}_L \\ \mathbf{D}_{RI}\mathbf{D}_{II}^{-1}\mathbf{F}_I + (\mathbf{D}_{RL} + \mathbf{D}_{RI}\mathbf{D}_{II}^{-1}\mathbf{D}_{IL})\mathbf{q}_L + (\mathbf{D}_{RR} + \mathbf{D}_{RI}\mathbf{D}_{II}^{-1}\mathbf{D}_{IR})\mathbf{q}_R &= \mathbf{F}_R\end{aligned}$$

That in matrix form become:

$$\begin{bmatrix} \bar{\mathbf{D}}_{LI}\mathbf{F}_I \\ \bar{\mathbf{D}}_{RI}\mathbf{F}_I \end{bmatrix} + \begin{bmatrix} \bar{\mathbf{D}}_{LL} & \bar{\mathbf{D}}_{LR} \\ \bar{\mathbf{D}}_{RL} & \bar{\mathbf{D}}_{RR} \end{bmatrix} \begin{bmatrix} \mathbf{q}_L \\ \mathbf{q}_R \end{bmatrix} = \begin{bmatrix} \mathbf{F}_L \\ \mathbf{F}_R \end{bmatrix} \quad (2.7)$$

Where,

$$\begin{aligned}\bar{\mathbf{D}}_{LL} &= \mathbf{D}_{LL} - \mathbf{D}_{LI}\mathbf{D}_{II}^{-1}\mathbf{D}_{IL} \\ \bar{\mathbf{D}}_{LR} &= \mathbf{D}_{LR} - \mathbf{D}_{RI}\mathbf{D}_{II}^{-1}\mathbf{D}_{IL} \\ \bar{\mathbf{D}}_{RL} &= \mathbf{D}_{RL} - \mathbf{D}_{RI}\mathbf{D}_{II}^{-1}\mathbf{D}_{IL} \\ \bar{\mathbf{D}}_{RR} &= \mathbf{D}_{RR} - \mathbf{D}_{RI}\mathbf{D}_{II}^{-1}\mathbf{D}_{IR} \\ \bar{\mathbf{D}}_{LI} &= \mathbf{D}_{LI}\mathbf{D}_{II}^{-1} \\ \bar{\mathbf{D}}_{RI} &= \mathbf{D}_{RI}\mathbf{D}_{II}^{-1}\end{aligned}$$

Considering two consecutive substructure ( $n$ ) and ( $n+1$ ) like in Figure (2.3), two fundamental conditions must be always satisfied:

- **continuity** of the displacement along the junction:

$$\mathbf{q}_R^{(n)} = \mathbf{q}_L^{(n+1)} \quad (2.8)$$

- **equilibrium** of the forces acting in the junction:

$$\mathbf{F}_R^{(n)} + \mathbf{F}_L^{(n+1)} = \mathbf{F}_B^{(n)} \quad (2.9)$$

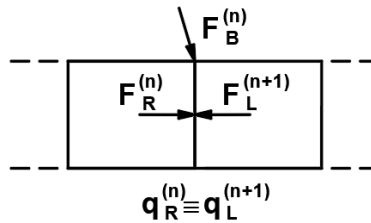


Figure 2.3: Forces and displacements between two consecutive substructures

The vector  $\mathbf{F}_B^{(n)}$  represents the *external nodal forces* applied to the right bound of the substructure ( $n$ ). Assuming that equation (2.7) holds for the substructure ( $n$ ), the application of the latter conditions gives:

$$\begin{bmatrix} \bar{\mathbf{D}}_{LI}\mathbf{F}_I^{(n)} \\ \bar{\mathbf{D}}_{RI}\mathbf{F}_I^{(n)} \end{bmatrix} + \begin{bmatrix} \bar{\mathbf{D}}_{LL} & \bar{\mathbf{D}}_{LR} \\ \bar{\mathbf{D}}_{RL} & \bar{\mathbf{D}}_{RR} \end{bmatrix} \begin{bmatrix} \mathbf{q}_L^{(n)} \\ \mathbf{q}_L^{(n+1)} \end{bmatrix} = \begin{bmatrix} \mathbf{F}_L^{(n)} \\ \mathbf{F}_B^{(n)} - \mathbf{F}_L^{(n+1)} \end{bmatrix} \quad (2.10)$$

These equations can be manipulated in order to write the terms regarding substructure ( $n+1$ ) in function of those regarding the preceding substructure ( $n$ ). From the first equation,

$$\mathbf{q}_L^{(n+1)} = -\bar{\mathbf{D}}_{LR}^{-1}\bar{\mathbf{D}}_{LL}\mathbf{q}_L^{(n)} + \bar{\mathbf{D}}_{LR}^{-1}\mathbf{F}_L^{(n)} - \bar{\mathbf{D}}_{LR}^{-1}\bar{\mathbf{D}}_{LI}\mathbf{F}_I^{(n)} \quad (2.11)$$

and from the second,

$$-\mathbf{F}_L^{(n+1)} = \bar{\mathbf{D}}_{RL}\mathbf{q}_L^{(n)} + \bar{\mathbf{D}}_{RR}\mathbf{q}_L^{(n+1)} + \bar{\mathbf{D}}_{RI}\mathbf{F}_I^{(n)} - \mathbf{F}_B^{(n)} \quad (2.12)$$

Replacing equation (2.11) in equation (2.12),

$$\begin{aligned} -\mathbf{F}_L^{(n+1)} = & (\bar{\mathbf{D}}_{RL} - \bar{\mathbf{D}}_{RR}\bar{\mathbf{D}}_{LR}^{-1}\bar{\mathbf{D}}_{LL})\mathbf{q}_L^{(n)} + \bar{\mathbf{D}}_{RR}\bar{\mathbf{D}}_{LR}^{-1}\mathbf{F}_L^{(n)} + \\ & + (\bar{\mathbf{D}}_{RI} - \bar{\mathbf{D}}_{RR}\bar{\mathbf{D}}_{LR}^{-1}\bar{\mathbf{D}}_{LI})\mathbf{F}_I^{(n)} - \mathbf{F}_B^{(n)} \end{aligned} \quad (2.13)$$

Equations (2.11) and (2.12) can be written in matrix form as:

$$\begin{bmatrix} \mathbf{q}_L^{(n+1)} \\ -\mathbf{F}_L^{(n+1)} \end{bmatrix} = \mathbf{S} \begin{bmatrix} \mathbf{q}_L^{(n)} \\ -\mathbf{F}_L^{(n)} \end{bmatrix} + \begin{bmatrix} \bar{\mathbf{D}}_{qI}\mathbf{F}_I^{(n)} \\ \bar{\mathbf{D}}_{fI}\mathbf{F}_I^{(n)} - \mathbf{F}_B^{(n)} \end{bmatrix} \quad (2.14)$$

Where,  $\mathbf{S}$  is the *transfer matrix* given by:

$$\mathbf{S} = \begin{bmatrix} -\bar{\mathbf{D}}_{LR}^{-1}\bar{\mathbf{D}}_{LL} & -\bar{\mathbf{D}}_{LR}^{-1} \\ \bar{\mathbf{D}}_{LR} - \bar{\mathbf{D}}_{RR}\bar{\mathbf{D}}_{LR}^{-1}\bar{\mathbf{D}}_{LL} & -\bar{\mathbf{D}}_{RR}\bar{\mathbf{D}}_{LR}^{-1} \end{bmatrix} \quad (2.15)$$

and,

$$\bar{\mathbf{D}}_{qI} = \bar{\mathbf{D}}_{LR}^{-1}\bar{\mathbf{D}}_{LI} \quad (2.16)$$

$$\bar{\mathbf{D}}_{fI} = \bar{\mathbf{D}}_{RI} - \bar{\mathbf{D}}_{RR}\bar{\mathbf{D}}_{LR}^{-1}\bar{\mathbf{D}}_{LI} \quad (2.17)$$

The nodal displacements  $\mathbf{q}^{(n)}$  and the nodal forces  $\mathbf{F}^{(n)}$ , together describe the state of the substructure. For this reason we define the *state vector* of the substructure ( $n$ ) as:

$$\mathbf{u}^{(n)} = \begin{bmatrix} \mathbf{q}^{(n)} \\ \mathbf{F}^{(n)} \end{bmatrix} \quad (2.18)$$

Finally, denoting with  $\mathbf{b}^{(n)}$  the vector of external loads acting on the substructure ( $n$ ) as:

$$\mathbf{b}^{(n)} = \begin{bmatrix} \bar{\mathbf{D}}_{qI} \mathbf{F}_I^{(n)} \\ \bar{\mathbf{D}}_{fI} \mathbf{F}_I^{(n)} - \mathbf{F}_B^{(n)} \end{bmatrix} \quad (2.19)$$

equation (2.14) can be written in a more synthetic form:

$$\mathbf{u}^{(n+1)} = \mathbf{S} \mathbf{u}^{(n)} + \mathbf{b}^{(n)} \quad (2.20)$$

This last equation represent the relation between the generic substructure ( $n$ ) and its next substructure ( $n + 1$ ) by means of the transfer matrix  $\mathbf{S}$  that will be examined in the next section.

## 2.2 Wave analysis

As introduced in the first chapter, the propagation constants and the wave shapes correspond to respectively the eigenvalue and eigenvector of matrix  $\mathbf{S}$ . Once the wave base is obtained, it'll be possible decompose the structure response on it. The *Transfer Matrix*  $\mathbf{S}$  relates the state vectors of two consecutive substructure. It has been obtained in terms of dynamic stiffness matrix and therefore represents a characteristic of the structure.

Its dimension is reduced compared to the DSM. In fact, reminding that each bound of the substructure presents  $d$  DOFs and each sub-matrix in  $\mathbf{S}$  has dimension  $d \times d$ , it follows that  $\mathbf{S}$  is also a square matrix and its dimension is  $2d \times 2d$ . Hence the number of eigenvalues and eigenvector will be  $2d$  and as will be demonstrated corresponds to  $d$  positive-going waves and  $d$  negative-going waves.

The free wave propagation is described by the eigenvalue problem:

$$\mathbf{S} \begin{bmatrix} \mathbf{q}_L \\ \mathbf{F}_L \end{bmatrix} = \mu_i \begin{bmatrix} \mathbf{q}_L \\ \mathbf{F}_L \end{bmatrix} \quad (2.21)$$

Where the eigenvector associated with the eigenvalue  $\mu_i$  is denoted by:

$$\phi_i = \begin{bmatrix} \mathbf{q}(\mu_i) \\ \mathbf{F}(\mu_i) \end{bmatrix} \quad (2.22)$$

The eigenvectors  $\phi_i$  compose the *wave base* of the structure:

$$\Phi = [\Phi_1 \quad \dots \quad \Phi_{2d}] \quad (2.23)$$

Comparing equation (1.5) with equation (2.21), it is possible to obtain the relation between the eigenvalue  $\mu_i$  and the propagation constant  $\beta_i$ :

$$\mu_i = e^{\beta_i} \quad (2.24)$$

### 2.2.1 Property of wave vectors

The wave vectors have properties that herein will be explained and commented.

The first row of equation (2.21) gives:

$$\mathbf{F}_L = -(\bar{\mathbf{D}}_{LL} + \mu\bar{\mathbf{D}}_{LR})\mathbf{q}_L \quad (2.25)$$

while, from the second row of the same equation:

$$(\bar{\mathbf{D}}_{LR} - \bar{\mathbf{D}}_{RR}\bar{\mathbf{D}}_{LR}^{-1}\bar{\mathbf{D}}_{LL})\mathbf{q}_L - \bar{\mathbf{D}}_{RR}\bar{\mathbf{D}}_{LR}^{-1}\mathbf{F}_L = \mu\mathbf{F}_L \quad (2.26)$$

By combining the previous two equation we obtain:

$$\left(\bar{\mathbf{D}}_{RR} + \bar{\mathbf{D}}_{LL} + \mu\bar{\mathbf{D}}_{LR} + \frac{1}{\mu}\bar{\mathbf{D}}_{RL}\right)\mathbf{q}_L = 0 \quad (2.27)$$

The vector  $\mathbf{q}_L$ , that represents the eigenvector corresponding to the eigenvalue  $\mu$ , is thus the solution of a quadratic eigenvalue problem.

Taking the transpose of equation (2.27), observing that for the symmetry of the dynamic stiffness matrix  $\bar{\mathbf{D}}_{LR}^T = \bar{\mathbf{D}}_{RL}$ ,  $\bar{\mathbf{D}}_{LL}^T = \bar{\mathbf{D}}_{LL}$  and  $\bar{\mathbf{D}}_{RR}^T = \bar{\mathbf{D}}_{RR}$ , and reminding the basic property of matrices  $(AB)^T = B^T A^T$ , we have:

$$\mathbf{q}_L^T \left(\bar{\mathbf{D}}_{RR} + \bar{\mathbf{D}}_{LL} + \mu\bar{\mathbf{D}}_{LR} + \frac{1}{\mu}\bar{\mathbf{D}}_{RL}\right) = 0 \quad (2.28)$$

Hence,  $\mathbf{q}_L$  is both a *right-eigenvector* associated to the eigenvalue  $\mu$  and a *left-eigenvector* associated with the eigenvalue  $1/\mu$ . Since the left and right eigenproblems have identical eigenvalues it follows that if  $\mu$  is an eigenvalue of equation (2.27), the same is true for  $1/\mu$ . The relative eigenvector represent a pair of positive and negative-going waves and this is true for any shape or property of the cell.

The eigenvector relative to the eigenvalue  $\mu_i$ , are:

$$\Phi_i = \begin{bmatrix} \mathbf{q}(\mu_i) \\ \mathbf{F}(\mu_i) \end{bmatrix} = \begin{bmatrix} \Phi_{q,i} \\ \Phi_{F,i} \end{bmatrix} \quad (2.29)$$

while the eigenvector relative to the eigenvalue  $\mu_i^* = 1/\mu_i$ , are

$$\Phi_i^* = \begin{bmatrix} \mathbf{q}(\mu_i^*) \\ \mathbf{F}(\mu_i^*) \end{bmatrix} = \begin{bmatrix} \Phi_{q,i}^* \\ \Phi_{F,i}^* \end{bmatrix} \quad (2.30)$$

## Orthogonality property

The orthogonality property can be demonstrated in the following way. We firstly rewrite the eigenvalue problem for two different eigenvector:

$$\begin{aligned}\mathbf{S}\phi_j &= \mu_j\phi_j \\ \phi_i^*\mathbf{S} &= \mu_i\phi_i^*\end{aligned}\tag{2.31}$$

Left multiplying the first equation for  $\phi_i^*$  and right multiplying the second for  $\phi_j$ , we have:

$$\phi_i^*\mathbf{S}\phi_j = \mu_j\phi_i^*\phi_j = \mu_i\phi_i^*\phi_j\tag{2.32}$$

This quantity must equal to zero if  $\mu_j \neq \mu_i$ , and so

$$\phi_i^*\phi_j = d_i\delta_{ij}\tag{2.33}$$

Where  $d_i$  is some constant and  $\delta_{ij}$  is the *Kronecker delta*. Finally orthogonality of the positive and negative eigenvalue has been demonstrated.

## 2.2.2 Solution of the eigenvalue problem

For a large number of degrees of freedom, direct use of usual numerical solvers can lead to difficulties because the transfer matrix can be ill-conditioned. To avoid this problem Zhong [10] considering that  $\mathbf{S}$  is a *symplectic* matrix, proposes to solve the problem in a different way.

In mathematics, a symplectic matrix is a  $2d \times 2d$  matrix that satisfies the condition:

$$\mathbf{S}^T\mathbf{J}\mathbf{S} = \mathbf{J}\tag{2.34}$$

where  $\mathbf{J}$  is a fixed  $2d \times 2d$  non-singular, skew-symmetric matrix,

$$\mathbf{J} = \begin{bmatrix} 0 & \mathbf{I}_d \\ -\mathbf{I}_d & 0 \end{bmatrix}\tag{2.35}$$

and  $\mathbf{I}_d$  is the  $d \times d$  identity matrix.

The eigenvalues of a symplectic matrix come in pairs hence the strategy of Zhong consisted in solving the problem in term of the eigenvalue  $\lambda_i = \mu_i + 1/\mu_i$ . This means that we search the eigenvalues of  $\mathbf{S} + \mathbf{S}^{-1}$  instead of the eigenvalues of  $\mathbf{S}$ . The eigenvalue problem to solve is:

$$\left[ (\mathbf{N}'\mathbf{J}\mathbf{L}'^T + \mathbf{L}'\mathbf{J}\mathbf{N}'^T) - \lambda_i\mathbf{L}'\mathbf{J}\mathbf{L}'^T \right] \mathbf{z}_i = \mathbf{0}\tag{2.36}$$

where:

$$\mathbf{L}' = \begin{bmatrix} 0 & \mathbf{I}_d \\ \mathbf{D}_{LR} & 0 \end{bmatrix}, \quad \mathbf{N}' = \begin{bmatrix} \mathbf{D}_{RL} & 0 \\ -(\mathbf{D}_{LL} + \mathbf{D}_{RR}) & -\mathbf{I}_d \end{bmatrix}\tag{2.37}$$

Once the eigenvalue are computed, the wave parameters ( $\mu_i, \mu_i^* = 1/\mu_i$ ) can be found analytically solving a quadratic equation of the form:

$$x^2 - \lambda_i x + 1 = 0, \quad \text{with } x \equiv \mu_i \quad (2.38)$$

The corresponding eigenvectors are obtained by the closed-form expressions:

$$\phi_i = \begin{bmatrix} \mathbf{I}_n & \mathbf{0} \\ \mathbf{D}_{RR} & \mathbf{I}_n \end{bmatrix} \mathbf{w}'_i, \quad \phi_i^* = \begin{bmatrix} \mathbf{I}_n & \mathbf{0} \\ \mathbf{D}_{RR} & \mathbf{I}_n \end{bmatrix} \mathbf{w}'_{i^*}, \quad (2.39)$$

Where

$$\mathbf{w}'_i = \mathbf{J}(\mathbf{L}'^T - \mu_i^* \mathbf{N}'^T) \mathbf{z}_i \quad (2.40)$$

$$\mathbf{w}'_{i^*} = \mathbf{J}(\mathbf{L}'^T - \mu_i \mathbf{N}'^T) \mathbf{z}_i \quad (2.41)$$

The eigenvalues  $\mu_i, \mu_i^*$  and the respective eigenvectors  $\phi_i, \phi_i^*$ , according to Bloch's theorem, are referred to *wave parameters* and *wave shapes*. The wave shapes express the way in which the junction between two substructure deforms.

Finally the wave base  $\{\Phi, \Phi^*\}$  of the transformation  $\mathbf{S}$  is obtained, where:

$$\Phi = [\phi_1 \quad \dots \quad \phi_d] \quad (2.42)$$

$$\Phi^* = [\phi_1^* \quad \dots \quad \phi_d^*] \quad (2.43)$$

Separating the components of the wave base corresponding to displacements  $\mathbf{q}$  and forces  $\mathbf{F}$ ,

$$\Phi = \begin{bmatrix} \Phi_q \\ \Phi_F \end{bmatrix} \quad \Phi^* = \begin{bmatrix} \Phi_q^* \\ \Phi_F^* \end{bmatrix} \quad (2.44)$$

and

$$\mu = \begin{bmatrix} \mu_1 & & & \\ & \mu_2 & & \\ & & \ddots & \\ & & & \mu_d \end{bmatrix} \quad \mu^* = \begin{bmatrix} \mu_1^* & & & \\ & \mu_2^* & & \\ & & \ddots & \\ & & & \mu_d^* \end{bmatrix} \quad (2.45)$$

We define, therefore, two sets of  $d$  eigenvalues and eigenvectors denoted by  $\{(\mu_i, \phi_i)\}$  and  $\{(\mu_i^*, \phi_i^*)\}$ , with the first set such that  $|\mu_j| \leq 1$ .

Depending on  $|\mu_j|$  we can split the waves into:

- Propagative waves for  $|\mu_j| = 1$
- Non-propagative waves<sup>1</sup> for  $|\mu_j| < 1$ .

---

<sup>1</sup>Waves which amplitude decreases travelling along the structure

### 2.2.3 Physical meaning of wave-modes

It has been demonstrated that two family of waves exist:

- Positive-going waves

$$\{(\mu_i, \phi_i)\} \quad \text{for} \quad |\mu_i| < 1$$

- Negative-going waves

$$\{(\mu_i^*, \phi_i^*)\} \quad \text{for} \quad |\mu_i^*| > 1$$

The eigenvalues  $\mu_i$  play the role of *structural damping* factor of a periodic structure. Consider the generic substructure in Figure (2.4):

- For positive-going wave (from left to right):

$$\mathbf{u}^{(n+1)} = \mu_i \mathbf{u}^{(n)} \implies \mathbf{u}^{(n+1)} < \mathbf{u}^{(n)}$$

- For negative-going wave (from right to left):

$$\mathbf{u}^{(n+1)} = \mu_i^* \mathbf{u}^{(n)} \implies \mathbf{u}^{(n+1)} > \mathbf{u}^{(n)}$$

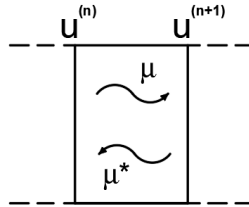
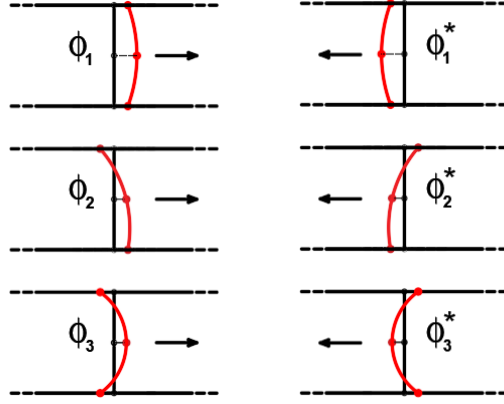


Figure 2.4: Wave parameters for right-going and left-going waves

The wave shapes can be seen as the possible way in which the coupling section can deform. If we consider a coupling section <sup>2</sup> consisting of three nodes and focus the attention only to the horizontal degree of freedom, it's easy to understand that the shapes that the section can take are those of Figure (2.5).

<sup>2</sup>For coupling section we consider the common edge between two consecutive substructures



(a) Wave shape for positive-going wave. (b) Wave shape for negative-going waves.

Figure 2.5: Wave shape of a coupling section made of three nodes with respect to the horizontal displacement

## 2.3 Approaches of the WFE method and analysis of a complete structure

### 2.3.1 Wave Amplitude (WA) approach

The wave base, refers to an infinitely periodic structure. Assuming a linear dynamic behaviour of the structure, the vibrations can be summed up linearly along the structure. Under this hypothesis, the superposition principle can be applied and it allows to describe the dynamic behaviour of a structure with a finite number of substructure through a pair of infinitely periodic structures [9]. Thus we can decompose the state vector  $\mathbf{u}^{(n)}$  and the load vector  $\mathbf{b}^{(n)}$  in the wave base as a combination of positive and negative waves:

$$\mathbf{u}^{(n)} = \Phi \mathbf{Q}^{(n)} - \Phi^* \mathbf{Q}^{*(n)} \quad (2.46)$$

$$\mathbf{b}^{(n)} = \Phi \mathbf{Q}_B^{(n)} - \Phi^* \mathbf{Q}_B^{*(n)} \quad (2.47)$$

Where  $\mathbf{Q}^{(n)}$  and  $\mathbf{Q}^{*(n)}$  represent the vectors of *wave amplitude* of the positive-going and negative-going waves. The minus sign denotes the different direction of the waves. In Figure (2.6) we note how the wave shape  $\phi_1$  and the respective propagation constant  $\mu_1$  are always the same while the *wave amplitude*  $\mathbf{Q}_1^{(n)}$  changes for every substructure due to the damping action of the propagation constant  $\mu_1$ .

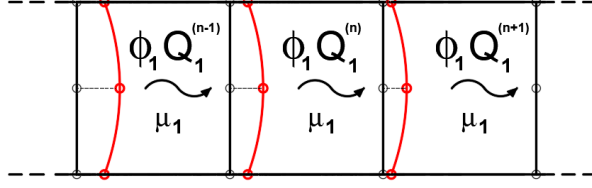


Figure 2.6: Wave amplitudes

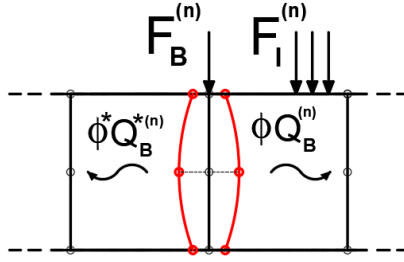


Figure 2.7: Wave amplitudes generated by the external loads.

The terms  $\mathbf{Q}_B^{(n)}$  and  $\mathbf{Q}_B^{*(n)}$  are the vectors of wave amplitude generated by the external loads  $\mathbf{F}_I^{(n)}$  and  $\mathbf{F}_B^{(n)}$  represented in Figure (2.7).

### Computation of $\mathbf{Q}_B$ and $\mathbf{Q}_B^*$

The wave amplitude of the external loads can be derived from equation (2.47), by multiplying both sides for  $\Phi^{*T} \mathbf{J}$  as follow:

$$\Phi^{*T} \mathbf{J} \mathbf{b}^{(n)} = \Phi^{*T} \mathbf{J} \Phi \mathbf{Q}_B^{(n)} + \Phi^{*T} \mathbf{J} \Phi^* \mathbf{Q}_B^{*(n)} \quad (2.48)$$

Being  $\Phi^{*T} \mathbf{J} \Phi^* = \mathbf{0}$ , we obtain:

$$\mathbf{Q}_B^{(n)} = \frac{\Phi^{*T} \mathbf{J} \mathbf{b}^{(n)}}{\Phi^{*T} \mathbf{J} \Phi} \quad (2.49)$$

The same thing can be done to compute the value of  $\mathbf{Q}_B^{*(k)}$ . Multiplying both sides for  $\Phi^T \mathbf{J}$ :

$$\Phi^T \mathbf{J} \mathbf{b}^{(n)} = \Phi^T \mathbf{J} \Phi \mathbf{Q}_B^{(n)} + \Phi^T \mathbf{J} \Phi^* \mathbf{Q}_B^{*(n)} \quad (2.50)$$

As before, being  $\Phi^T \mathbf{J} \Phi = \mathbf{0}$ , we have:

$$\mathbf{Q}_B^{*(n)} = \frac{\Phi^T \mathbf{J} \mathbf{b}^{(n)}}{\Phi^T \mathbf{J} \Phi^*} \quad (2.51)$$

Developing the numerator of equations (2.49) and (2.51) we have:

$$\Phi^{*T} \mathbf{J} \mathbf{b}^{(n)} = (\Phi_q^{*T} \mathbf{D}_{fI} - \Phi_F^{*T} \mathbf{D}_{qI}) \mathbf{F}_I^{(k)} - \Phi_q^{*T} \mathbf{F}_B^{(k)} \quad (2.52)$$

$$\Phi^T \mathbf{J} \mathbf{b}^{(n)} = (\Phi_q^T \mathbf{D}_{fI} - \Phi_F^T \mathbf{D}_{qI}) \mathbf{F}_I^{(k)} - \Phi_q^T \mathbf{F}_B^{(k)} \quad (2.53)$$

It can be demonstrated [1] that the relation between  $\Phi_q$  and  $\Phi_F$  is given by:

$$\Phi_F = \mathbf{D}_{RR} \Phi_q + \mathbf{D}_{RL} \Phi_q \boldsymbol{\mu}^* = -(\mathbf{D}_{LL} \Phi_q + \mathbf{D}_{LR} \Phi_q \boldsymbol{\mu}) \quad (2.54)$$

$$\Phi_F^* = \mathbf{D}_{RR} \Phi_q^* + \mathbf{D}_{RL} \Phi_q^* \boldsymbol{\mu} = -(\mathbf{D}_{LL} \Phi_q^* + \mathbf{D}_{LR} \Phi_q^* \boldsymbol{\mu}^*) \quad (2.55)$$

By substituting equations (2.16), (2.17), (2.54) and (2.55) in equations (2.52) and (2.53) we have:

$$\Psi \mathbf{Q}_B^{(k)} = (\boldsymbol{\mu} \Phi_q^{*T} \mathbf{D}_{LI} + \Phi_q^{*T} \mathbf{D}_{RI}) \mathbf{F}_I^{(k)} + \Phi_q^{*T} \mathbf{F}_B^{(k)} \quad (2.56)$$

$$\Psi^* \mathbf{Q}_B^{*(k)} = (\boldsymbol{\mu}^* \Phi_q^T \mathbf{D}_{LI} + \Phi_q^T \mathbf{D}_{RI}) \mathbf{F}_I^{(k)} + \Phi_q^T \mathbf{F}_B^{(k)} \quad (2.57)$$

Where  $\Psi$  and  $\Psi^*$  represent the *weighting matrix* given by:

$$\Psi = \Phi^{*T} \mathbf{J} \Phi \quad (2.58)$$

$$\Psi^* = \Phi^T \mathbf{J} \Phi^* \quad (2.59)$$

These matrices, will normalize the wave base, avoiding the influence of the ill-conditioned matrix on the orthogonality of the eigenvectors.

Is important to remark that:

$$\Psi^* = -\Psi^T \quad (2.60)$$

### Analysis of a complete structure

Once the relation between two consecutive substructures is known and the wave base has been computed, we can analyse a complete periodic structure. Consider the periodic structure in Figure (2.8) composed by  $N$  substructure.

Recalling equation (2.20) and developing the expression for  $n = 0, 1, 2$  we obtain:

- $n = 0 \implies \mathbf{u}^{(1)} = \mathbf{S} \mathbf{u}^{(0)} + \mathbf{b}^{(0)}$
- $n = 1 \implies \mathbf{u}^{(2)} = \mathbf{S} \mathbf{u}^{(1)} + \mathbf{b}^{(1)} \implies \mathbf{u}^{(2)} = \mathbf{S}^2 \mathbf{u}^{(0)} + \mathbf{S} \mathbf{b}^{(0)} + \mathbf{b}^{(1)}$
- $n = 2 \implies \mathbf{u}^{(3)} = \mathbf{S} \mathbf{u}^{(2)} + \mathbf{b}^{(2)} \implies \mathbf{u}^{(3)} = \mathbf{S}^3 \mathbf{u}^{(0)} + \mathbf{S}^2 \mathbf{b}^{(0)} + \mathbf{S} \mathbf{b}^{(1)} + \mathbf{b}^{(2)}$

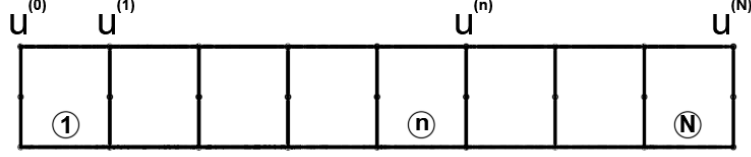


Figure 2.8: Periodic Structure composed by  $N$  substructures

This represent a *geometric series* [2]. For  $N$  elements:

$$\mathbf{u}^{(n)} = \mathbf{S}^n \mathbf{u}^{(0)} + \sum_{k=1}^n \mathbf{S}^{n-k} \mathbf{b}^{(k-1)} \quad (2.61)$$

The term  $\mathbf{b}^{(k-1)}$  refers to the left side of substructure ( $k$ ). From now on we'll refer to  $\mathbf{b}^{(k)}$  which represent the load vector referred to the substructure ( $n$ ). Equation (2.61) represents the relation between the state vector of the first substructure and the state vector of the generic substructure ( $n$ ).

Is possible, with some algebra, to obtain the relation between the last state vector and a generic one:

$$\mathbf{u}^{(N)} = \mathbf{S}^{N-n} \mathbf{u}^{(n)} + \sum_{k=n+1}^{N-1} \mathbf{S}^{N-k} \mathbf{b}^{(k)} \quad (2.62)$$

Placing equations (2.46) and (2.47) in equation (2.62) the relations between the wave amplitudes are given by:

$$\mathbf{Q}^{(n)} = \mu^n \mathbf{Q} + \sum_{k=1}^n \mu^{n-k} \mathbf{Q}_B^{(k)} \quad (2.63)$$

$$\mathbf{Q}^{*(n)} = \mu^{N-n} \mathbf{Q}^* - \sum_{k=n+1}^{N-1} \mu^{k-n} \mathbf{Q}_B^{*(k)} \quad (2.64)$$

Where  $\mathbf{Q}$  and  $\mathbf{Q}^*$  represent the wave amplitude of the first and last substructure respectively.

To obtain equations (2.63) and (2.64), the general expression of the eigenvalue problem ( $\mathbf{S}\Phi = \Phi\mu$ ) and the orthogonality properties of the eigenvectors have been used.

Substituting equations (2.63) and (2.64) in the wave descomposition (2.46)

and (2.47), the state vector of a generic substructure can be written as [2]:

$$\mathbf{u}^{(n)} = \Phi \boldsymbol{\mu}^n \mathbf{Q} - \Phi^* \boldsymbol{\mu}^{N-n} \mathbf{Q}^* + \Phi \sum_{k=1}^n \boldsymbol{\mu}^{n-k} \mathbf{Q}_B^{(k)} + \Phi^* \sum_{k=n+1}^{N-1} \boldsymbol{\mu}^{k-n} \mathbf{Q}_B^{*(k)} \quad (2.65)$$

From which the nodal displacement are:

$$\mathbf{q}^{(n)} = \Phi_q \boldsymbol{\mu}^n \mathbf{Q} - \Phi_q^* \boldsymbol{\mu}^{N-n} \mathbf{Q}^* + \Phi_q \sum_{k=1}^n \boldsymbol{\mu}^{n-k} \mathbf{Q}_B^{(k)} + \Phi_q^* \sum_{k=n+1}^{N-1} \boldsymbol{\mu}^{k-n} \mathbf{Q}_B^{*(k)} \quad (2.66)$$

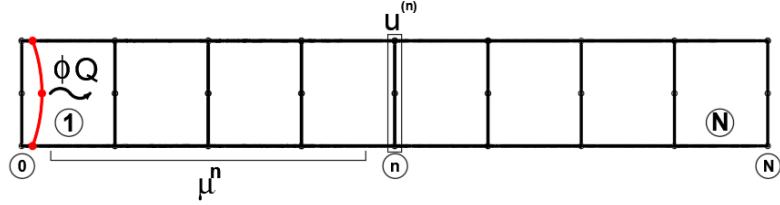
while the nodal forces are:

$$\mathbf{F}^{(n)} = \Phi_F \boldsymbol{\mu}^n \mathbf{Q} - \Phi_F^* \boldsymbol{\mu}^{N-n} \mathbf{Q}^* + \Phi_F \sum_{k=1}^n \boldsymbol{\mu}^{n-k} \mathbf{Q}_B^{(k)} + \Phi_F^* \sum_{k=n+1}^{N-1} \boldsymbol{\mu}^{k-n} \mathbf{Q}_B^{*(k)} \quad (2.67)$$

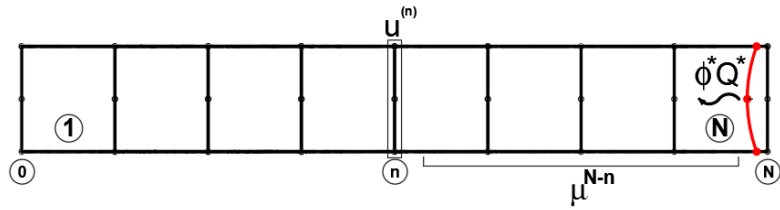
The only unknowns of expression (2.65) are the wave amplitude of the first substructure  $\mathbf{Q}$  and the last substructure  $\mathbf{Q}^*$ .

The application of the boundary condition at the ends of the structure, allow to compute this values and obtain the final response of the structure. Equation (3.32) is composed by four parts each of which has a clear meaning.

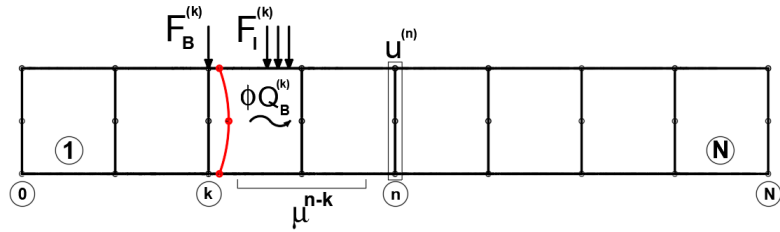
- $\Phi \boldsymbol{\mu}^n \mathbf{Q}$  represents the positive wave coming from the first substructure reduced by the propagation constant  $\boldsymbol{\mu}$  powered by  $n$  (note that  $\boldsymbol{\mu} < 1$ ), i.e. the number of substructures between the left end of the structure and the interested substructure (Figure 2.9a)
- $\Phi^* \boldsymbol{\mu}^{N-n} \mathbf{Q}^*$  represents the negative wave coming from the last substructure reduced by the propagation constant  $\boldsymbol{\mu}$  powered by  $N - n$ , i.e. the number of substructures between the right end of the entire structure and the interested substructure (Figure 2.9b)
- $\Phi \sum_{k=1}^n \boldsymbol{\mu}^{n-k} \mathbf{Q}_B^{(k)}$  is the sum of all the positive waves caused by the forces applied to the left of the substructure  $n$ , each of them reduced by the propagation constant  $\boldsymbol{\mu}$  powered by  $n - k$ , i.e. the number of substructures between every applied force and the interested point (Figure 2.9c)
- $\Phi^* \sum_{k=n+1}^{N-1} \boldsymbol{\mu}^{k-n} \mathbf{Q}_B^{*(k)}$  is the sum of all the positive waves caused by the forces applied to the right of the substructure  $n$ , each of them reduced by the propagation constant  $\boldsymbol{\mu}$  powered by  $k - n$ , i.e. the number of substructure between every applied force and the interested point (Figure 2.9d)



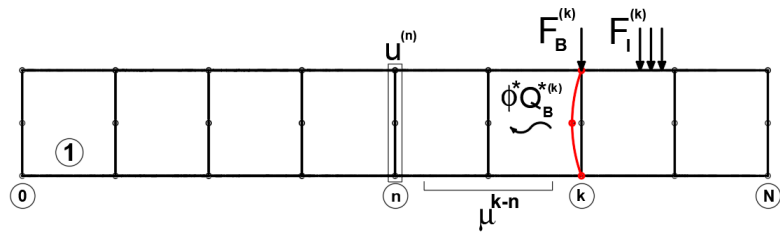
(a) Contribution 1. Wave amplitude of the first substructure reduced by the factor  $\mu^n$ .



(b) Contribution 2. Wave amplitude of the last substructure reduced by the factor  $\mu^{N-n}$ .



(c) Contribution 3. Wave amplitude caused by the external loads applied to substructure (k) reduced by the factor  $\mu^{n-k}$ .



(d) Contribution 4. Wave amplitude caused by the external loads applied to substructure (k) reduced by the factor  $\mu^{k-n}$ .

Figure 2.9: Graphic explanation of the state vector equation in terms of different contributions.

### 2.3.2 Dynamic stiffness matrix (DSM) approach

The DSM approach represents a different way to solve the entire structure. While the WA Approach gives the response of the structure in function of the wave amplitudes, the DSM Approach is based on deriving the total DSM of the structure starting from the one relative to a general substructure. In fact, the dynamic stiffness matrix of the complete structure, is built easily from the knowledge of wave modes and propagation constant calculated from one cell.

This approach gives a relation between nodal forces and the DOFs of left and right ends of the periodic structure in the form [1, 2]:

$$\begin{bmatrix} \mathbf{F}_L^{(0)} \\ \mathbf{F}_R^{(N)} \end{bmatrix} = \mathbf{D}_T \begin{bmatrix} \mathbf{q}_L^{(0)} \\ \mathbf{q}_R^{(N)} \end{bmatrix} + \mathbf{F}_T \quad (2.68)$$

Where  $\mathbf{D}_T$  and  $\mathbf{F}_T$  are the *equivalent dynamic stiffness matrix* and the *vector of external loads* applied on the structure given by [1]:

$$\mathbf{D}_T = \begin{bmatrix} \mathbf{D}_{LL} & \mathbf{0} \\ \mathbf{0} & \mathbf{D}_{RR} \end{bmatrix} + \begin{bmatrix} \Phi_q^{*-T} \boldsymbol{\mu}^N \Phi_q^{*T} & \mathbf{I} \\ \mathbf{I} & \Phi_q^{-T} \boldsymbol{\mu}^N \Phi_q^T \end{bmatrix}^{-1} \times \begin{bmatrix} \Phi_q^{*-T} \boldsymbol{\mu}^{N-1} \Phi_q^{*T} & \Phi_q^{*-T} \boldsymbol{\mu} \Phi_q^{*T} \\ \Phi_q^{-T} \boldsymbol{\mu} \Phi_q^T & \Phi_q^{-T} \boldsymbol{\mu}^{N-1} \Phi_q^T \end{bmatrix} \begin{bmatrix} \mathbf{D}_{LR} & \mathbf{0} \\ \mathbf{0} & \mathbf{D}_{RL} \end{bmatrix} \quad (2.69)$$

$$\mathbf{F}_T = \begin{bmatrix} \Phi_q^{*-T} \boldsymbol{\mu}^N \Phi_q^{*T} & \mathbf{I} \\ \mathbf{I} & \Phi_q^{-T} \boldsymbol{\mu}^N \Phi_q^T \end{bmatrix}^{-1} \times \sum_{k=1}^N \begin{bmatrix} \Phi_q^{*-T} \boldsymbol{\mu}^{N-k-1} \Phi_q^{*T} & \Phi_q^{*-T} \boldsymbol{\mu}^{N-k} \Phi_q^{*T} \\ \Phi_q^{-T} \boldsymbol{\mu}^{k+1} \Phi_q^T & \Phi_q^{-T} \boldsymbol{\mu}^k \Phi_q^T \end{bmatrix} \begin{bmatrix} \mathbf{D}_{LI} \mathbf{F}_I^{(k)} \\ \mathbf{D}_{RI} \mathbf{F}_I^{(k)} + \mathbf{F}_B^{(k)} \end{bmatrix} \quad (2.70)$$

Is possible to observe that the external loads give no contribution to the global matrix  $\mathbf{D}_T$  but lead to an equivalent load  $\mathbf{F}_T$  in the dynamic equation (2.68).

## 2.4 Application of the WA approach

Using the WA approach, a simply supported beam has been solved. This example is necessary to introduce the next chapter in order to understand which are the improvement and the differences.

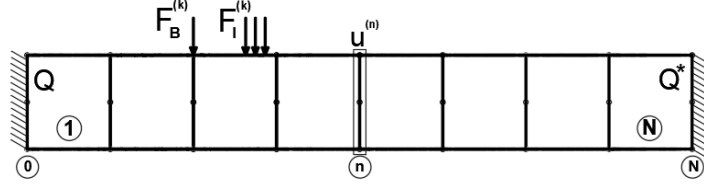


Figure 2.10: Periodic Structure composed by  $N$  substructures and fixed in both ends.

The structure considered is a fixed-fixed beam represented in Figure (2.10).

The boundary condition are:

$$\mathbf{q}^{(0)} = 0, \quad \mathbf{q}^{(N)} = 0 \quad (2.71)$$

Substituting the number of the substructure in equation (3.32) we obtain:

$$\Phi_q \mathbf{Q} - \Phi_q^* \mu^N \mathbf{Q}^* + \Phi_q^* \sum_{k=1}^{N-1} \mu^k \mathbf{Q}_B^{*(k)} = 0 \quad (2.72)$$

$$\Phi_q \mu^N \mathbf{Q} - \Phi_q^* \mathbf{Q}^* + \Phi_q \sum_{k=1}^N \mu^{N-k} \mathbf{Q}_B^{(k)} = 0 \quad (2.73)$$

The unknowns of the previous two equation are  $\mathbf{Q}$  and  $\mathbf{Q}^*$ . From equations (2.72) and (2.73), we have:

$$A = \begin{bmatrix} \Phi_q & -\Phi_q^* \mu^N \\ \Phi_q \mu^N & -\Phi_q^* \end{bmatrix} \quad (2.74)$$

$$F = \begin{bmatrix} \Phi_q^* \sum_{k=1}^{N-1} \mu^k \mathbf{Q}_B^{*(k)} \\ \Phi_q \sum_{k=1}^N \mu^{N-k} \mathbf{Q}_B^{(k)} \end{bmatrix} \quad (2.75)$$

Finally the wave amplitudes are given by:

$$\mathbf{Q} = A^{-1} F \quad (2.76)$$

Where:

$$\mathbf{Q} = \begin{bmatrix} \mathbf{Q} \\ \mathbf{Q}^* \end{bmatrix} \quad (2.77)$$

## Chapter 3

# New application of the WFEM

In the previous chapter the wave finite element method has been presented. Starting from the finite elements analysis of a generic sub-structure it's been possible to derive the dynamic behaviour of the whole structure. This method has been used to solve numerous structures but it can not deal easily with boundary conditions. In this chapter, a technique of WFE will be developed to deal with more general cases of structures constrained in a arbitrary manner as a multiple supported bridge. By using the WA approach, the vectors of DOF and nodal loads will be decomposed on the base wave in function of loads and reaction forces of the supports. Then by substituting the boundary condition in this wave decomposition, we obtain a relation between the reaction forces and the loads which permits to calculate the structure response. The first section is dedicated to the manipulation of the original expression of the WA approach in order to make explicit the reactions of the intermediate constrains. The second section aims to present an original method designed to make easier the application of the boundary conditions and finally in the third section will be constructed the linear system which represents the solution of the application.

### 3.1 Derivation of the intermediate reactions

The WA approach allows to compute the response of the entire structure applying the boundary conditions in order to obtain the unknowns  $\mathbf{Q}$  and  $\mathbf{Q}^*$ . In the application seen in Section (2.4) it has been sufficient to impose equal to zero all the displacements of the state vector at the two ends of the structure  $\mathbf{q}^{(0)}$  and  $\mathbf{q}^{(N)}$ . If it had been a cantilever, the other kind of condition would have been to impose all zero forces in the free end. These problems are of immediate solution, but if instead of a free or fixed extreme we were dealing with a pinned or a simple support, the situation is more complicated. Moreover, the presence of intermediate constraints in turn would increase the difficulties. In the case of extreme constraints, the boundary conditions should be imposed only to some components of the state vector. However the reactions to the constraints do not influence, in the calculation phase, the final response and can be easily obtained as they correspond to the force components of the state vector  $\mathbf{u}^{(0)}$  or  $\mathbf{u}^{(N)}$  unless external forces are applied to the ends of the structure. For intermediate constraints, the conditions must be applied only to the bounded nodes. Furthermore the reactions, besides being a priori unknown, will influence the final response of the structure. Hence, the first thing to do is to make explicit the reactions at intermediate constraints starting from the general expression of the state vector  $\mathbf{u}^{(n)}$ . In the presence of a constrain, the coupling conditions presented in section (2.1) must be modified. By convention, the constrain can be placed only in the junction between two substructures as showed in Figure (3.1). If we consider the reactions as external forces acting on the structure, from the equilibrium of external forces and internal forces we have:

$$\mathbf{F}_R^{(n)} + \mathbf{F}_L^{(n+1)} = \mathbf{F}_{ext}^{(n)} + \mathbf{R}^{(n)} \quad (3.1)$$

Hence this time  $\mathbf{F}_B$  is given by:

$$\mathbf{F}_B^{(k)} = \mathbf{F}_{ext}^{(k)} + \mathbf{R}^{(k)} \quad (3.2)$$

The wave amplitudes  $\mathbf{Q}_B^{(k)}$  and  $\mathbf{Q}_B^{*(k)}$  will be influenced by the reactions  $\mathbf{R}^{(n)}$ . Placing equation (3.2) in equation (2.56) and (2.57), the wave amplitude can be expressed in function of the external loads  $\mathbf{F}_{ext}^{(k)}$  and reactions  $\mathbf{R}^{(k)}$  as follow:

$$\mathbf{Q}_B^{(k)} = (\boldsymbol{\mu}\boldsymbol{\Phi}_q^{*T}\mathbf{D}_{LI} + \boldsymbol{\Phi}_q^{*T}\mathbf{D}_{RI})\mathbf{F}_I^{(k)} + \boldsymbol{\Phi}_q^{*T}(\mathbf{F}_{ext}^{(k)} + \mathbf{R}^{(k)}) \quad (3.3)$$

$$\mathbf{Q}_B^{*(k)} = (\boldsymbol{\mu}^*\boldsymbol{\Phi}_q^T\mathbf{D}_{LI} + \boldsymbol{\Phi}_q^T\mathbf{D}_{RI})\mathbf{F}_I^{(k)} + \boldsymbol{\Phi}_q^T(\mathbf{F}_{ext}^{(k)} + \mathbf{R}^{(k)}) \quad (3.4)$$

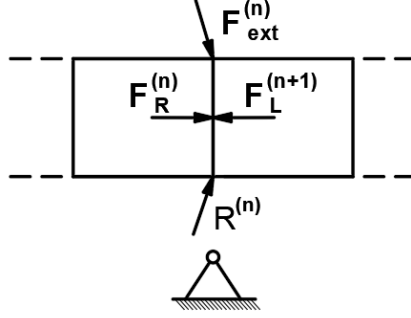


Figure 3.1: Equilibrium between two consecutive substructure in proximity of a constrain.

We can rewrite the equation (3.32), splitting the sums in order to isolate respectively the external forces and the reaction at the supports,

$$\begin{aligned}
\mathbf{u}^{(n)} = & \Phi \boldsymbol{\mu}^n \mathbf{Q} - \Phi^* \boldsymbol{\mu}^{N-n} \mathbf{Q}^* + \Phi \sum_{k=1}^n \boldsymbol{\mu}^{n-k} \Theta^* \mathbf{F}_I^{(k)} + \Phi^* \sum_{k=n+1}^N \boldsymbol{\mu}^{k-n} \Theta \mathbf{F}_I^{(k)} \\
& + \Phi \sum_{k=1}^n \boldsymbol{\mu}^{n-k} \Phi_q^{*T} \mathbf{F}_{ext}^{(k)} + \Phi^* \sum_{k=n+1}^N \boldsymbol{\mu}^{k-n} \Phi_q^T \mathbf{F}_{ext}^{(k)} \\
& + \Phi \sum_{k=1}^n \boldsymbol{\mu}^{n-k} \Phi_q^{*T} \mathbf{R}^{(k)} + \Phi^* \sum_{k=n+1}^N \boldsymbol{\mu}^{k-n} \Phi_q^T \mathbf{R}^{(k)} \quad (3.5)
\end{aligned}$$

where:

$$\Theta = \boldsymbol{\mu} \Phi_q^{*T} \mathbf{D}_{LI} + \Phi_q^{*T} \mathbf{D}_{RI} \quad (3.6)$$

$$\Theta^* = \boldsymbol{\mu}^* \Phi_q^T \mathbf{D}_{LI} + \Phi_q^T \mathbf{D}_{RI} \quad (3.7)$$

The only non-zero terms of the sum in which appear the vector  $\mathbf{R}^{(k)}$  are those where exists a constrain. If we call  $\mathbf{R}^{(n_s)}$  the vector of reaction corresponding to the constrain  $s$  placed in  $n_s$ , then the sum can be modified as follow:

$$\begin{aligned}
\mathbf{u}^{(n)} = & \Phi \boldsymbol{\mu}^n \mathbf{Q} - \Phi^* \boldsymbol{\mu}^{N-n} \mathbf{Q}^* + \mathbf{T}^{(n)} + \\
& + \Phi \sum_{s, n_s \leq n} \boldsymbol{\mu}^{n-n_s} \Phi_q^{*T} \mathbf{R}^{(n_s)} + \Phi^* \sum_{s, n_s > n}^S \boldsymbol{\mu}^{n_s-n} \Phi_q^T \mathbf{R}^{(n_s)} \quad (3.8)
\end{aligned}$$

Where  $\mathbf{T}^{(n)}$  gathers all the known terms and is given by:

$$\mathbf{T}^{(n)} = \mathbf{T}_I^{(n)} + \mathbf{T}_{ext}^{(n)} \quad (3.9)$$

where,

$$\mathbf{T}_I^{(n)} = \Phi \sum_{k=1}^n \mu^{n-k} \Theta^* \mathbf{F}_I^{(k)} + \Phi^* \sum_{k=n+1}^N \mu^{k-n} \Theta \mathbf{F}_I^{(k)} \quad (3.10)$$

$$\mathbf{T}_{ext}^{(n)} = \Phi \sum_{k=1}^n \mu^{n-k} \Phi_q^{*T} \mathbf{F}_{ext}^{(k)} + \Phi^* \sum_{k=n+1}^N \mu^{k-n} \Phi_q^T \mathbf{F}_{ext}^{(k)} \quad (3.11)$$

## 3.2 Boundary conditions

Once the reactions at the intermediate supports are explicit is necessary to apply the boundary conditions at each constrain.

Consider a periodic structure composed of  $N$  substructures and  $S$  constrains as showed in Figure (3.2).

Each support can be identified by the index  $s$  such that  $s \in [1, S]$ , where each corresponding substructure is denoted by:

$$n_1 \dots n_s \dots n_S.$$

The first and the last supports of the periodic structure, are assumed to be located to the beginning and the end of the periodic structure (Figure 3.2). This leads to:

$$n_1 = 0 \quad \text{and} \quad n_S = N$$

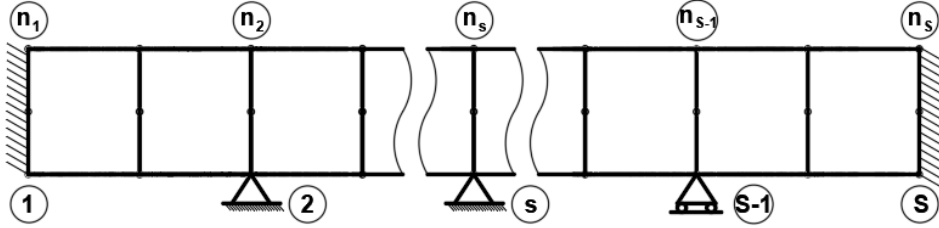


Figure 3.2: General structure with different type of constrains

The intermediate constrains can be placed everywhere. Indeed, the periodicity of the structure doesn't influence their position. Moreover the number and the type of support are arbitrary. To explain the strategy utilized to apply the boundary condition, a simple case will be shown.

Consider a one dimensional beam. Each node has three DOF, therefore the state vector  $\mathbf{u}^{(n)}$  is defined as:

$$\mathbf{u}^{(n)} = \begin{bmatrix} \mathbf{q}^{(n)} \\ \mathbf{F}^{(n)} \end{bmatrix} = \begin{bmatrix} \mathbf{q}_1^{(n)} \\ \mathbf{q}_2^{(n)} \\ \mathbf{q}_3^{(n)} \\ \mathbf{F}_1^{(n)} \\ \mathbf{F}_2^{(n)} \\ \mathbf{F}_3^{(n)} \end{bmatrix}$$

Where the subscripts 1,2 and 3 designate the vertical, horizontal and rotational degree of freedom respectively.

For a *pinned support*, the vertical and horizontal displacement, together with the momentum of the forces are zero:

$$\begin{cases} \mathbf{q}_1^{(n)} = 0 \\ \mathbf{q}_2^{(n)} = 0 \\ \mathbf{F}_3^{(n)} = 0 \end{cases}$$

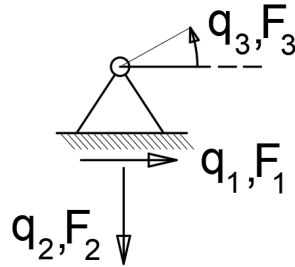


Figure 3.3: Pinned support

The same result can be reached multiplying the state vector for a index matrix and put the result equal to a zero vector:

$$\begin{bmatrix} 1 & 0 & 0 & 0 & 0 & 0 \\ 0 & 1 & 0 & 0 & 0 & 0 \\ 0 & 0 & 0 & 0 & 0 & 1 \end{bmatrix} \begin{bmatrix} \mathbf{q}_1^{(n)} \\ \mathbf{q}_2^{(n)} \\ \mathbf{q}_3^{(n)} \\ \mathbf{F}_1^{(n)} \\ \mathbf{F}_2^{(n)} \\ \mathbf{F}_3^{(n)} \end{bmatrix} = \begin{bmatrix} \mathbf{q}_1^{(n)} \\ \mathbf{q}_2^{(n)} \\ \mathbf{F}_3^{(n)} \end{bmatrix} = \begin{bmatrix} 0 \\ 0 \\ 0 \end{bmatrix}$$

If we denote the index matrix with  $\mathbf{L}_s$  and call the zero vector the vector of boundary conditions  $\mathbf{B}_s$ , the application of the conditions can be written in the more synthetic way:

$$\mathbf{L}_s \mathbf{u}^{(n_s)} = \mathbf{B}_s \quad (3.12)$$

It is easy to understand that by changing the position of the ones in matrix  $\mathbf{L}_s$ , we can refer to different types of constraints. It is important to make a fundamental distinction between extreme constraints, those at the ends of the structure, and intermediate constraints. From this distinction, in fact, the  $\mathbf{L}_s$  matrix will assume different dimensions even for the same constraint. At the extremes of the structure it is possible to impose conditions both on displacements and on forces. In fact, unless external forces are applied to the extremes, the forces acting on the unconstrained nodes are null. It is possible therefore to impose conditions on them. In the case of intermediate constraints, the conditions can only be placed in the constrained nodes whose value necessarily equals the vector  $\mathbf{B}_s$ . On the unconstrained nodes, on the other hand, it is not possible to impose conditions on the forces as these are different from zero because they represent the means by which the wave motion is transmitted from one element to another. For this reason the boundary conditions will be imposed only for the displacements that are dual of the reactions. In the next paragraph a more general definition of the matrix  $\mathbf{L}$  is given.

### 3.2.1 Index matrix $\mathbf{L}$

The matrix  $\mathbf{L}$  is a *logical matrix* or *(0, 1) matrix* which elements belong to the Boolean domain  $\mathbb{B} = \{0, 1\}$ . It can assume different form depending on the type of constraint and his position along the structure.

In accordance with the previous section, the constraints are divided in two general types: *extreme constraints* for  $s = 1$  and  $s = S$ , and *intermediate constraints* for  $s \in [2, S - 1]$ .

For a one-dimensional beam, the extreme support is represented by a index matrix  $\mathbf{L}_s$  with 3 *rows* and 6 *columns*.

Hence, for  $\mathbf{L}_1$  and  $\mathbf{L}_S$  we can have:

- Fixed support:

$$\begin{bmatrix} 1 & 0 & 0 & 0 & 0 & 0 \\ 0 & 1 & 0 & 0 & 0 & 0 \\ 0 & 0 & 1 & 0 & 0 & 0 \end{bmatrix}$$

- Pinned support:

$$\begin{bmatrix} 1 & 0 & 0 & 0 & 0 & 0 \\ 0 & 1 & 0 & 0 & 0 & 0 \\ 0 & 0 & 0 & 0 & 0 & 1 \end{bmatrix}$$

- Roller support:

$$\begin{bmatrix} 0 & 1 & 0 & 0 & 0 & 0 \\ 0 & 0 & 0 & 1 & 0 & 0 \\ 0 & 0 & 0 & 0 & 0 & 1 \end{bmatrix}$$

For the intermediate supports the number of rows depends on the type of support.

We define the matrix  $\mathbf{L}_s$  for  $s = 2 \dots (S - 1)$  as:

- Fixed support:

$$\begin{bmatrix} 1 & 0 & 0 \\ 0 & 1 & 0 \\ 0 & 0 & 1 \end{bmatrix}$$

- Pinned support:

$$\begin{bmatrix} 1 & 0 & 0 \\ 0 & 1 & 0 \end{bmatrix}$$

- Roller support:

$$[0 \quad 1 \quad 0]$$

The number of rows represent the number of equation and the number of unknown reaction.

The index matrix  $\mathbf{L}_s$  for two-dimensional and three-dimensional structures is not so easy to find like for 1D structures and needs to be assembled because of the incremented number on nodes in the junction (see Figure 3.4). For the extreme constrains the matrix  $\mathbf{L}_s$  has always the same number of rows and columns and in particular, the rows match with the components' number  $d$  of vector  $\mathbf{Q}$  (or  $\mathbf{Q}^*$ ) and the columns match with the components' number of the state vector  $\mathbf{u}^{(n)}$  correspond to  $2d$ . Remind that  $d$  is the number of DOFs of the boundary nodes of a generic substructure  $n$ . For a complex substructure (2D or 3D),  $\mathbf{L}_s$  could reach large dimensions. The strategy used is to construct the matrix  $\mathbf{L}_s$  by means of sub-matrices that subsequently can be assembled. For multiple node junctions, the column state vector is composed by the  $d$  nodal displacements followed by the  $d$  nodal forces.

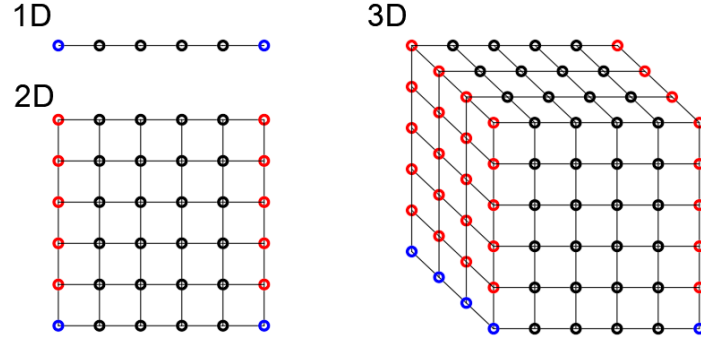


Figure 3.4: Different type of junction depending on the dimension of the structure. The blue nodes represent those in which the intermediate constrain are placed

The Matrix  $\mathbf{L}_s$ , that multiplies the state vector (see equation 3.12) can be seen as the composition of two square sub-matrix  $\mathbf{L}_q$  and  $\mathbf{L}_F$  that apply to displacements and forces respectively:

$$\mathbf{L}_s \mathbf{u}^{(n_s)} = \left[ \begin{array}{c|c} \mathbf{L}_q & \mathbf{L}_F \end{array} \right] \begin{bmatrix} \{\mathbf{q}\} \\ \{\mathbf{F}\} \end{bmatrix} \quad (3.13)$$

The matrices  $\mathbf{L}_q$  and  $\mathbf{L}_F$ , in turn, consist of sub-matrices, corresponding to each node, named  $\mathbf{L}_{q,sub}$  and  $\mathbf{L}_{F,sub}$ . These sub-matrix are square, identical for every node and depend on the kind of support. Their dimension correspond to the number of DOF for each node.

$$\mathbf{L}_q = \begin{bmatrix} \mathbf{L}_{q,sub} & & & \\ & \ddots & & \\ & & \mathbf{L}_{q,sub} & \\ & & & \ddots \\ & & & & \mathbf{L}_{q,sub} \end{bmatrix} \quad (3.14)$$

$$\mathbf{L}_F = \begin{bmatrix} \mathbf{L}_{F,sub} & & & \\ & \ddots & & \\ & & \mathbf{L}_{F,sub} & \\ & & & \ddots \\ & & & & \mathbf{L}_{F,sub} \end{bmatrix} \quad (3.15)$$

The sub-matrices  $\mathbf{L}_{q,sub}$  and  $\mathbf{L}_{F,sub}$  have to be constructed appositely for every type of structure (beam, shell, plates, etc.) from whom the number of

DOF per node depends.

The matrix  $\mathbf{L}_s$  for intermediate constrains corresponds to  $\mathbf{L}_q$  since the conditions are only applied to the displacement. For the intermediate supports the number of rows depends on the type of support and will change with it. While the number of columns is always the same and correspond to  $d$ .

Finally, the composition of matrix  $\mathbf{L}_s$  depends by:

- Type of constrain (roller support, pinned support, fixed support)
- Dimension of the structure (1D, 2D, 3D)
- DOF per each node
- Position along the structure:
  - to the ends (extreme)
  - between the ends (intermediate)

### 3.2.2 Vector of boundary conditions $\mathbf{B}$

The boundary conditions are denoted by the column vector  $\mathbf{B}_s$ , where the subscript refers to the respective constrain  $s$ . Each component represents the admitted displacement of each DOF. The vector  $\mathbf{B}_s$  depend on the type of constrain, for:

- rigid constrains:  $\mathbf{B}_s = [\mathbf{0}]$
- elastic constrain:  $\mathbf{B}_s \neq [\mathbf{0}]$

## 3.3 Solution of the problem

In order to apply the boundary conditions, equation (3.8) has to be multiplied for the index matrix  $\mathbf{L}_s$  and equalled to the vector  $\mathbf{B}_s$ .

For each support  $s$ , the boundary conditions can be written as:

$$\begin{cases} \mathbf{B}_s = \mathbf{L}_s \mathbf{u}^{(n_s)} & \text{for } s = 1, s = S \\ \mathbf{B}_s = \mathbf{L}_s \mathbf{q}^{(n_s)} & \text{for } s \in [2, S - 1] \end{cases} \quad (3.16)$$

so that:

$$\begin{aligned} & \mathbf{L}_s \Phi \boldsymbol{\mu}^{n_s} \mathbf{Q} - \mathbf{L}_s \Phi^* \boldsymbol{\mu}^{N-n_s} \mathbf{Q}^* + \mathbf{L}_s \mathbf{T}^{(n_s)} + \\ & + \mathbf{L}_s \Phi \sum_{i=2}^s \boldsymbol{\mu}^{n_s-n_i} \Phi_q^{*T} \mathbf{R}^{(n_i)} + \mathbf{L}_s \Phi^* \sum_{i=s+1}^{S-1} \boldsymbol{\mu}^{n_i-n_s} \Phi_q^T \mathbf{R}^{(n_i)} = \mathbf{B}_s \end{aligned} \quad (3.17)$$

For intermediate constrains the terms  $\Phi$  and  $\Phi^*$  are replaced by  $\Phi_q$  and  $\Phi_q^*$ . The next step consists in replacing the vector  $\mathbf{R}^{(n_i)}$  with the expression  $\mathbf{L}_i^T \tilde{\mathbf{R}}^{(n_i)}$  in order to consider only the non zero components of the reaction. Moving all the known terms of Equation (3.17) to the right side of the equation, we have:

$$\begin{aligned} & \mathbf{L}_s \Phi \boldsymbol{\mu}^{n_s} \mathbf{Q} + \mathbf{L}_s \Phi \sum_{i=2}^s \boldsymbol{\mu}^{n_s-n_i} (\mathbf{L}_i \Phi_q^*)^T \tilde{\mathbf{R}}^{(n_i)} + \\ & + \mathbf{L}_s \Phi^* \sum_{i=s+1}^{S-1} \boldsymbol{\mu}^{n_i-n_s} (\mathbf{L}_i \Phi_q)^T \tilde{\mathbf{R}}^{(n_i)} - \mathbf{L}_s \Phi^* \boldsymbol{\mu}^{N-n_s} \mathbf{Q}^* = \mathbf{B}_s - \mathbf{L}_s \mathbf{T}^{(n_s)} \end{aligned} \quad (3.18)$$

For a notation issue, the following assumption are made:

$$\Phi_s = \mathbf{L}_s \Phi; \quad \Phi_s^* = \mathbf{L}_s \Phi^* \quad \text{for } s = 1, s = S \quad (3.19)$$

$$\Phi_s = \mathbf{L}_s \Phi_q; \quad \Phi_s^* = \mathbf{L}_s \Phi_q^* \quad \text{for } 2 < s < S - 1 \quad (3.20)$$

Finally:

$$\begin{aligned} & \Phi_s \boldsymbol{\mu}^{n_s} \mathbf{Q} + \Phi_s \sum_{i=2}^s \boldsymbol{\mu}^{n_s-n_i} \Phi_i^{*T} \tilde{\mathbf{R}}^{(n_i)} + \\ & + \Phi_s^* \sum_{i=s+1}^{S-1} \boldsymbol{\mu}^{n_i-n_s} \Phi_i^T \tilde{\mathbf{R}}^{(n_i)} - \Phi_s^* \boldsymbol{\mu}^{N-n_s} \mathbf{Q}^* = \mathbf{B}_s - \mathbf{L}_s \mathbf{T}^{(n_s)} \end{aligned} \quad (3.21)$$

### 3.3.1 Definition of the linear system

Equation (3.21) can be written for every constrain  $s$ , leading to a system of linear equation in the form:

$$\mathbf{A}\mathbf{X} = \mathbf{F} \quad (3.22)$$

Where:

- $\mathbf{A}$  is the coefficient matrix.
- $\mathbf{X}$  is the unknown vector.
- $\mathbf{F}$  is the vector of known terms.

### Coefficient matrix, $\mathbf{A}$

The matrix  $\mathbf{A}$  is obtained from the left member of equation (3.21). The first row correspond to the first constrain. For  $s = 1$ ,

$$\Phi_1 \mathbf{Q} + \Phi_1^* \sum_{i=2}^{S-1} \mu^{n_i} \Phi_i^T \tilde{\mathbf{R}}^{(n_i)} - \Phi_s^* \mu^N \mathbf{Q}^*$$

The  $(S - 2)$  rows, corresponding to the intermediate constrains, are:

$$\Phi_s \mu^{n_s} \mathbf{Q} + \Phi_s \sum_{i=2}^s \mu^{n_s - n_i} \Phi_i^* \tilde{\mathbf{R}}^{(n_i)} + \Phi_s^* \sum_{i=s+1}^{S-1} \mu^{n_i - n_s} \Phi_i^T \tilde{\mathbf{R}}^{(n_i)} - \Phi_s^* \mu^{N - n_s} \mathbf{Q}^*$$

Is important to remark that, in this case, the elements of the sum change along the row  $s$ .

The last row corresponds to the last constrain. For  $s = S$ ,  $n_s = N$  hence:

$$\Phi_S \mu^N \mathbf{Q} + \Phi_S \sum_{i=2}^S \mu^{N - n_i} \Phi_i^* \tilde{\mathbf{R}}^{(n_i)} - \Phi_S^* \mathbf{Q}^*$$

Finally the matrix  $\mathbf{A}$  is:

$$\mathbf{A} = \begin{bmatrix} \Phi_1 & \cdots & \Phi_1^* \mu^{n_s} \Phi_s^T & \cdots & -\Phi_1^* \mu^N \\ \vdots & \ddots & \vdots & \vdots & \vdots \\ \Phi_s \mu^{n_s} & \cdots & \Phi_s \Phi_s^* & \cdots & -\Phi_s^* \mu^{N - n_s} \\ \vdots & \vdots & \vdots & \ddots & \vdots \\ \Phi_S \mu^N & \cdots & \Phi_S \mu^{N - n_s} \Phi_s^* & \cdots & -\Phi_S^* \end{bmatrix} \quad (3.23)$$

The matrix  $\mathbf{A}$  is a square matrix and this will allow us to invert it and solve the linear system.

### Unknown vector, $\mathbf{X}$

From the construction of matrix  $\mathbf{A}$  results that the vector of the unknowns is:

$$\mathbf{X} = \begin{bmatrix} \mathbf{Q} \\ \tilde{\mathbf{R}}^{(n_2)} \\ \vdots \\ \tilde{\mathbf{R}}^{(n_s)} \\ \vdots \\ \tilde{\mathbf{R}}^{(n_{S-1})} \\ \mathbf{Q}^* \end{bmatrix} \quad (3.24)$$

### Vector of known terms

The vector  $\mathbf{F}$  is defined as:

$$\mathbf{F} = \mathbf{B} - \mathbf{T}$$

With:

$$\mathbf{B} = \begin{bmatrix} \mathbf{B}^{(n_1)} \\ \vdots \\ \mathbf{B}^{(n_s)} \\ \vdots \\ \mathbf{B}^{(n_s)} \end{bmatrix} \quad \mathbf{T} = \begin{bmatrix} \mathbf{T}^{(n_1)} \\ \vdots \\ \mathbf{T}^{(n_s)} \\ \vdots \\ \mathbf{T}^{(n_s)} \end{bmatrix}$$

$\mathbf{B}$  is the general Boundary vector that gathers all the boundary conditions for every constrained node.

The vector  $\mathbf{T}$  can be decomposed in the sum of two parts:

$$\mathbf{T} = \mathbf{H}_I \mathbf{F}_I + \mathbf{H}_{ext} \mathbf{F}_{ext} \quad (3.25)$$

The column vector  $\mathbf{F}_I$  represents the external forces acting on the internal nodes of each substructure, while  $\mathbf{F}_{ext}$  represents the column vector of external forces acting at the boundary nodes of each substructure. They are given by:

$$\mathbf{F}_I = \begin{bmatrix} \mathbf{F}_I^{(1)} \\ \vdots \\ \mathbf{F}_I^{(n)} \\ \vdots \\ \mathbf{F}_I^{(N)} \end{bmatrix} \quad \mathbf{F}_{ext} = \begin{bmatrix} \mathbf{F}_{ext}^{(1)} \\ \vdots \\ \mathbf{F}_{ext}^{(n)} \\ \vdots \\ \mathbf{F}_{ext}^{(N)} \end{bmatrix} \quad (3.26)$$

Note that each element represents in turn a vector composed by the forces applied in each direction for every node considered.

The matrices  $\mathbf{H}_I$  and  $\mathbf{H}_{ext}$  are derived from equations (3.10) and (3.11) respectively. Multiplying equation (3.10) for the respective matrix  $\mathbf{L}_s$  we obtain:

$$\mathbf{L}_s \Phi \sum_{k=1}^{n_s} \mu^{n_s-k} \Theta^* \mathbf{F}_I^{(k)} + \mathbf{L}_s \Phi^* \sum_{k=n_s+1}^N \mu^{k-n_s} \Theta \mathbf{F}_I^{(k)} \quad (3.27)$$

and applying this equation for every support:

$$\mathbf{H}_I = \begin{bmatrix} \Phi_1^* \mu \Theta & \dots & \Phi_1^* \mu^n \Theta & \dots & \Phi_1^* \mu^N \Theta \\ \vdots & \vdots & \vdots & \vdots & \vdots \\ \Phi_s \mu^{n_s-1} \Theta^* & \dots & \Phi_s \Theta^* & \dots & \Phi_s^* \mu^{N-n_s} \Theta \\ \vdots & \vdots & \vdots & \vdots & \vdots \\ \Phi_S \mu^{N-1} \Theta^* & \dots & \Phi_S \mu^{N-n} \Theta^* & \dots & \Phi_S \Theta^* \end{bmatrix} \quad (3.28)$$

Doing the same for equation (3.11):

$$\mathbf{L}_s \Phi \sum_{k=1}^{n_s} \boldsymbol{\mu}^{n_s-k} \Phi_q^{*T} \mathbf{F}_{ext}^{(k)} + \mathbf{L}_s \Phi^* \sum_{k=n_s+1}^N \boldsymbol{\mu}^{k-n_s} \Phi_q^T \mathbf{F}_{ext}^{(k)} \quad (3.29)$$

and writing it for every constrain we derive the matrix  $\mathbf{H}_{ext}$  given by:

$$\mathbf{H}_{ext} = \begin{bmatrix} \Phi_1^* \boldsymbol{\mu} \Phi_q^T & \cdots & \Phi_1^* \boldsymbol{\mu}^n \Phi_q^T & \cdots & \Phi_1^* \boldsymbol{\mu}^N \Phi_q^T \\ \vdots & \vdots & \vdots & \vdots & \vdots \\ \Phi_s \boldsymbol{\mu}^{n_s-1} \Phi_q^{*T} & \cdots & \Phi_s \Phi_q^{*T} & \cdots & \Phi_s^* \boldsymbol{\mu}^{N-n_s} \Phi_q^T \\ \vdots & \vdots & \vdots & \vdots & \vdots \\ \Phi_S \boldsymbol{\mu}^{N-1} \Phi_q^{*T} & \cdots & \Phi_S \boldsymbol{\mu}^{N-n} \Phi_q^{*T} & \cdots & \Phi_S \Phi_q^{*T} \end{bmatrix} \quad (3.30)$$

Observe that both matrix  $\mathbf{H}_I$  and  $\mathbf{H}_{ext}$  are not square matrices.

### 3.3.2 Solution of the linear system

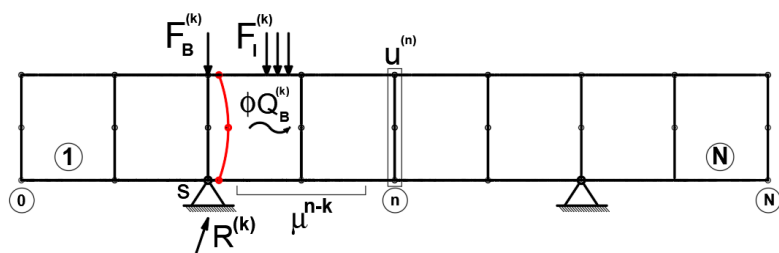
Once matrix  $\mathbf{A}$  and vector  $\mathbf{F}$  are defined, is possible to solve the problem:

$$\mathbf{X} = \mathbf{A}^{-1} \mathbf{F} \quad (3.31)$$

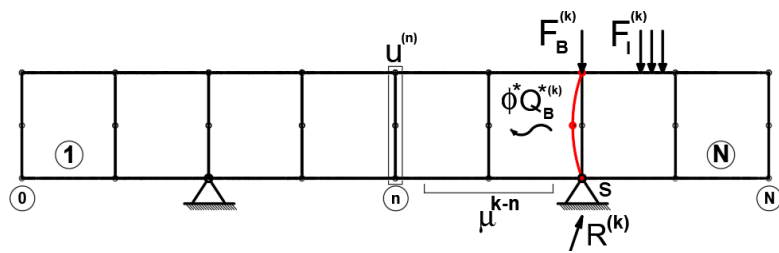
Replacing the reactions  $\mathbf{R}$  and wave amplitudes  $\mathbf{Q}$  and  $\mathbf{Q}^*$  in equation (3.8), the response of the entire periodic structure is obtained.

$$\mathbf{u}^{(n)} = \Phi \boldsymbol{\mu}^n \mathbf{Q} - \Phi^* \boldsymbol{\mu}^{N-n} \mathbf{Q}^* + \Phi \sum_{k=1}^n \boldsymbol{\mu}^{n-k} \mathbf{Q}_B^{(k-1)} + \Phi^* \sum_{k=n+1}^{N-1} \boldsymbol{\mu}^{k-n} \mathbf{Q}_B^{*(k-1)} \quad (3.32)$$

This time, the load amplitude depends also from the reactions of the intermediate constrain. In Figure (3.5) are represented the differences with respect to Figure (2.9).



(a) Wave amplitude caused by the external loads and the reaction applied to substructure (k) reduced by the factor  $\mu^{n-k}$ .



(b) Wave amplitude caused by the external loads and the reaction applied to substructure (k) reduced by the factor  $\mu^{k-n}$ .

Figure 3.5: Graphic explanation of the state vector equation with the influence of the reactions.

# Chapter 4

## Applications

In order to validate this technique, three applications have been developed. The three structures will present different dimensions and types of constraints placed in an arbitrary manner. In every application, the load is an impulse that in the time domain can be represented by a Dirac delta function and whose Fourier transform turns out to be a constant function in the frequency domain. For each application the frequency response function (FRF) of the structure will be calculated with respect to a specific point. The response in the time domain can in turn be obtained by means of an inverse Fourier transform. To confirm the results, every problem will be solved both by the FE method and the WFE method. Furthermore, for both methods the calculation time will be calculated so that the efficiency can be compared. The general procedure consists in dividing the structure into a certain number of identical substructures. Using the software Abaqus, the substructure is modelled and the stiffness and mass matrix obtained. By importing this data, the problem can be solved by the software Matlab. In fact, from the stiffness and mass matrix it is possible to obtain the dynamic stiffness matrix and the transfer matrix  $\mathbf{S}$ . Through the use of a specific Matlab function (written by D. Duhamel, Wave element library, 11/03/2014), the eigenvalue problem is solved the basis of vectors obtained for each frequency value. For the calculation of the structure a Matlab script has been specifically written that allows to set the boundary conditions (through the matrices  $\mathbf{L}_s$ ). The system (3.22) is automatically solved and the unknowns calculated. Finally, by applying the final expression of the WA approach, the response of the structure is obtained. Each application is divided into subsection. The first is to present the structure (geometry and physical characteristics), the boundary and loading conditions. The second is to show the characteristics of the numerical model of the substructure and finally, the results with relative comments.

## 4.1 1D Beam

### 4.1.1 Problem statement

The structure considered is the multi supported beam represented in Figure (4.13) with  $L = 50m$ . The objective of this application is to demonstrate the possibility of consider different type of constrained not necessarily equi-spaced.

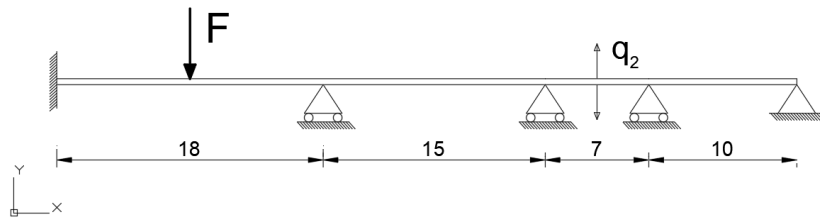


Figure 4.1: Multi-supported beam

The section of the beam is a IPE 400 (see Annex B). The external force is a vertical impulse and act to the middle of the first span. His value is  $F = 5kN$ . The material considered is steel and the mechanical properties are summarized in Table (4.1).

Steel	
Density	$d = 7850 \text{ kg/m}^3$
Elastic modulus	$E = 210 \text{ GPa}$
Poisson modulus	$\nu = 0.3$

Table 4.1: Mechanical properties of steel.

### 4.1.2 Description of the substructure

The beam is composed by 220 substructure of length  $l = 0.2m$ . The type of element is a 2-node linear beam in a plane. The information on the numerical model of the substructure and the entire substructure are summarized in (4.4). The substructure is represented in Figure (4.13).

	substructure	entire structure
number of elements	10	2200
number of nodes	11	2201
number of DOFs	33	6603

Table 4.2: Informations on the numerical model

### 4.1.3 Results and comments

In Figure (4.2) and (4.3) are reported the results of the analysis. The results match perfectly. The computational time is drastically reduced being 49.31s for FEM and 5.57s for WFEM.

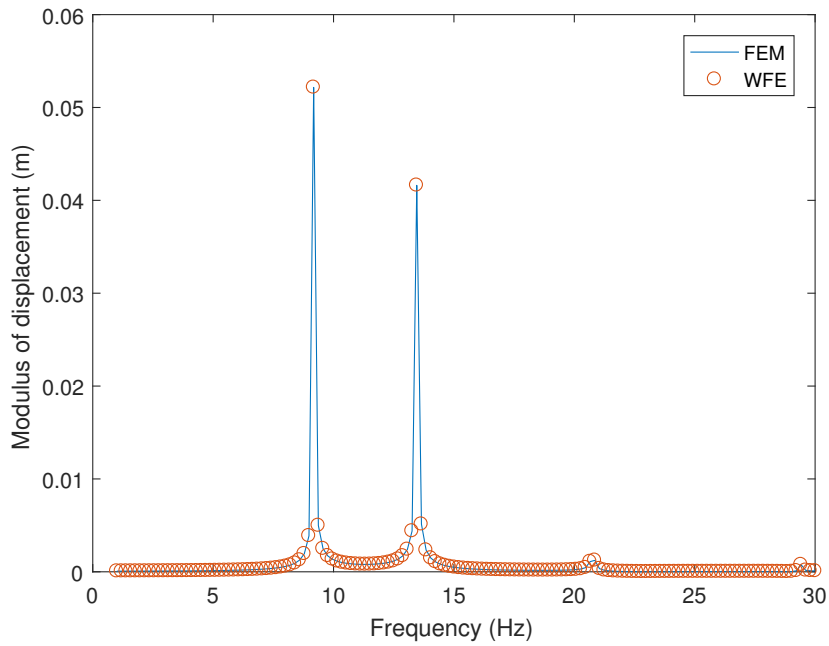


Figure 4.2: Frequency response function. Modulus of the displacement in function of the frequency.

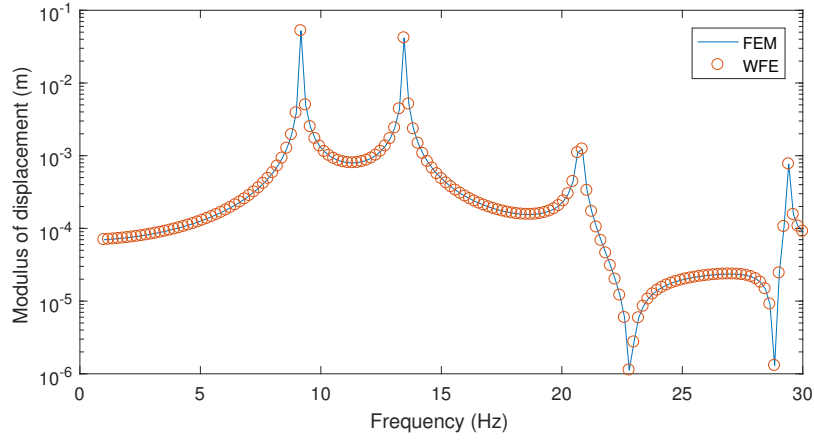


Figure 4.3: Frequency response function. Logarithm of the modulus of the displacement in function of the frequency.

## 4.2 2D Beam

### 4.2.1 Problem statement

The structure solved is multi-supported 2D beam of total length:  $L = 24m$ . In this application we're dealing with a plane stress problem. Two ends of the structure will be fixed while the others constrains are simple supports. The beam has a width of  $0.2 m$  and a thickness of  $0.01 m$ .

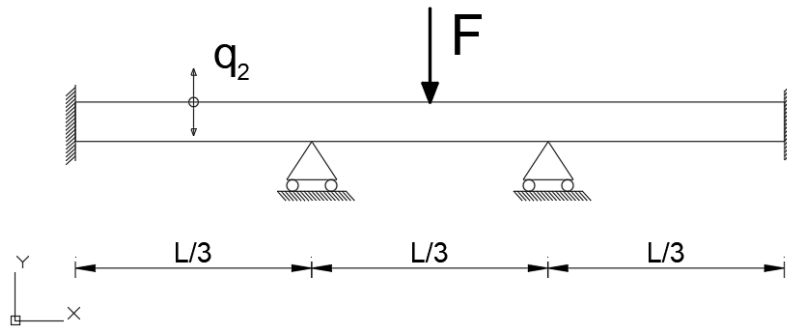


Figure 4.4: Multi-supported 2D beam

The external force is a vertical impulse and act to the middle of the structure. His value is  $F = 1 kN$ . The material considered is concrete and the mechanical properties are summarized in Table (4.3).

Concrete	
Density	$d = 2500 \text{ kg/m}^3$
Elastic modulus	$E = 31.5 \text{ GPa}$
Poisson modulus	$\nu = 0.2$

Table 4.3: Physical and Mechanical characteristic of concrete.

## 4.2.2 Description of the substructure

The beam is composed by 120 substructures of square dimension  $0.2m \times 0.2m$  and thickness  $0.01m$ . Using the FEM, the substructure's DMS is obtained considering a mesh of  $10 \times 10$  elements. The type of element is a 4-node bilinear plane stress quadrilateral.

	substructure	entire structure
number of elements	100	12000
number of nodes	121	13211
number of DOFs	242	26422

Table 4.4: Informations on the numerical model

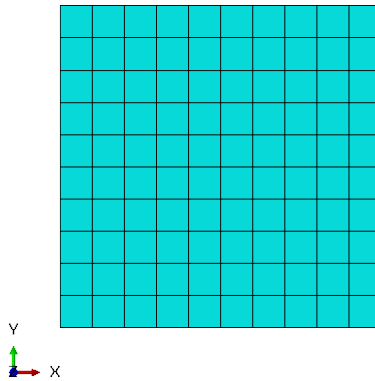


Figure 4.5: Model of the 2D substructure

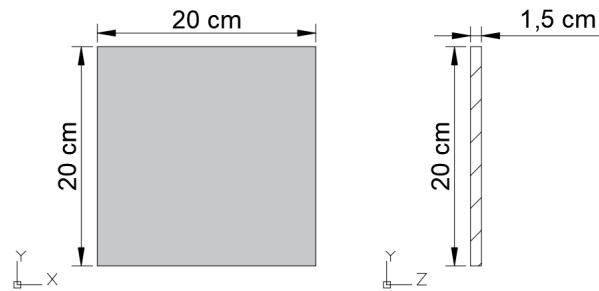


Figure 4.6: Geometrical characteristic of the substructure

### 4.2.3 Results and comments

The FRF has been computed relatively to the position indicated in Figure (4.4). The results are represented in Figure (4.7). Here again the WFEM has been faster than the FEM with 9.63s against 573.30s. The time reduction is of the 98%

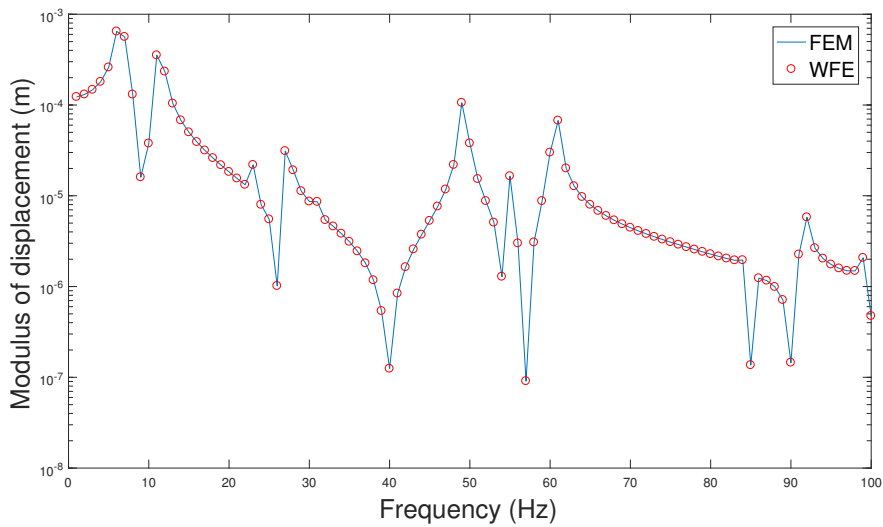


Figure 4.7: Frequency response function of the 2D beam calculated using the WFEM (o) compared to the FEM (-)

## 4.3 Multi-supported bridge

### 4.3.1 Description of the structure

In this section, the dynamic behaviour of a multi-supported bridge is studied. The total length is  $L = 120m$ . The bridge is fixed to the ends<sup>1</sup> and supported by two equispaced roller supports. The maximum span is  $L_{span} = 40m$ . The longitudinal scheme of the bridge is represented in Figure (4.8). The bridge

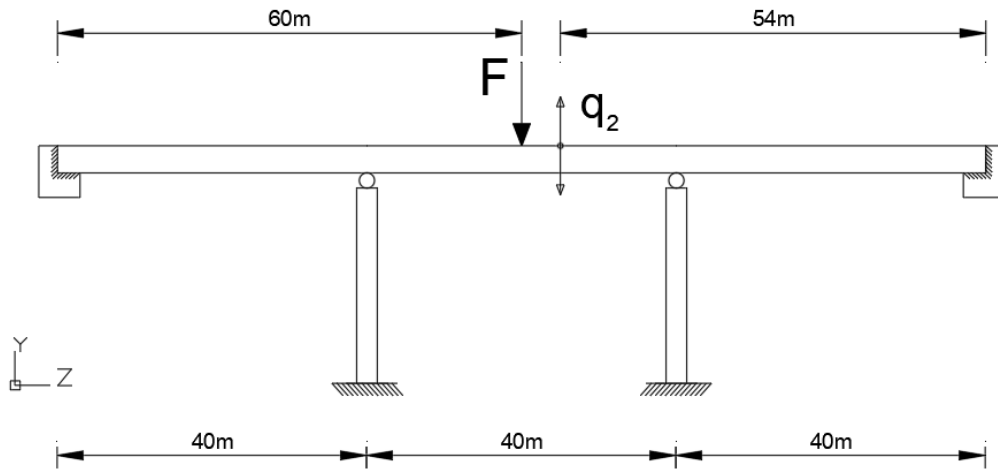


Figure 4.8: Multi-supported bridge

present a box-beam deck which dimensions are represented in Figure (4.9).

The external force is a vertical impulse and act to the middle of the structure; his value is  $F = 10 kN$ . The position is represented in Figure (4.10)a. The material considered is concrete and the mechanical property are summarized in Table (4.5). The position in which the displacements are assessed

HP Concrete	
Density	$d = 2500 kg/m^3$
Elastic modulus	$E = 48 GPa$
Poisson modulus	$\nu = 0.2$

Table 4.5: Physical and Mechanical characteristic of concrete.

is represented in Figure (4.10)b.

<sup>1</sup>The decision to fix the ends has been made in order to avoid numerical problems that appear when the matrix  $A$  is inverted.

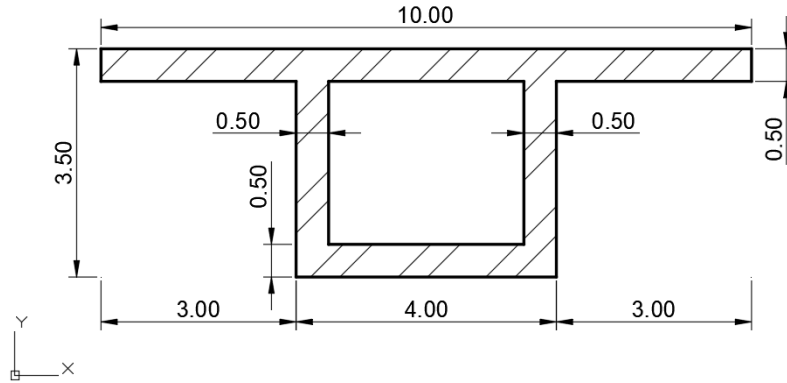
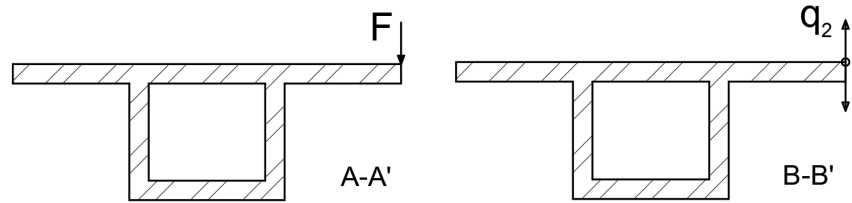


Figure 4.9: Section of the bridge ( $m$ ).



(a) Section A-A'. Point of application of the force.

(b) Section B-B'. Position of the computed displacements.

Figure 4.10: Sections in which are represented the application point of the external force and the response of the structure

### 4.3.2 Description of the substructure

The bridge is composed by 480 substructure of length  $l = 0.25m$ . The substructure has been modelled by a 8-node linear brick of dimensions  $0.25m$  represented in Figure (4.11)a. In Table (4.6) are summarized the informations about the numerical model of one substructure compared with the entire structure which model is showed in Figure (4.11)b.

	substructure	entire structure
number of elements	152	21280
number of nodes	456	109668
number of DOFs	1368	329004

Table 4.6: Information on the mesh

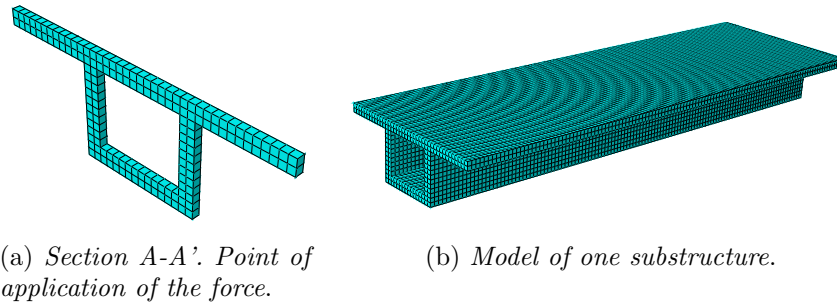


Figure 4.11: Model of the entire structure

### 4.3.3 Results and comments

The has been computed every  $0.15\text{ Hz}$  in a range the frequency of  $0 - 30\text{ Hz}$ . The result obtained by applying the WFE method matches with the one obtained with the FEM. Moreover the computational time is halved being 204 minutes for FEM and 100 minutes for WFEM equivalent to 51% of time reduction. The results are showed in Figure (4.12).

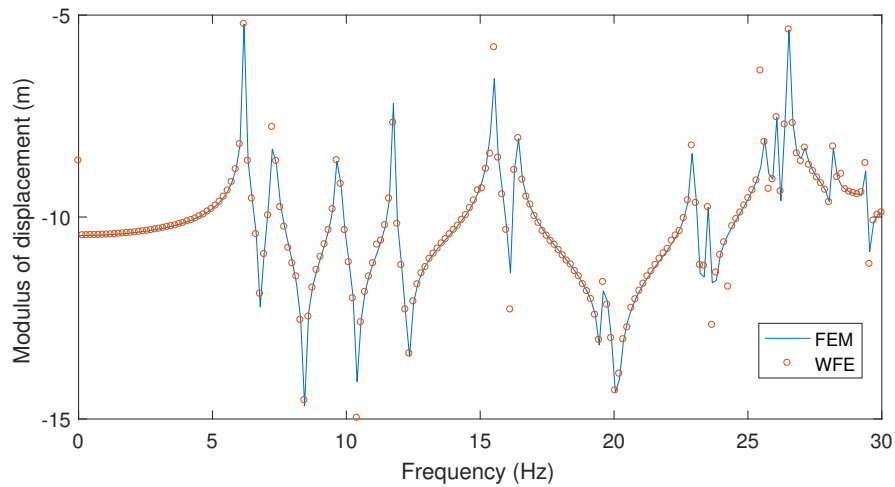


Figure 4.12: FRF of the bridge. Comparison between the WFEM (o) and the FEM (-)

## 4.4 General comments

As already mentioned, the WFE method has proved to be an excellent calculation tool to obtain results in a definitely shorter time compared to FEM. The proposed technique, that can be seen as a way to impose the boundary conditions, is simple but at the same time very effective. The precision of the results is very good with the exception of the application on the bridge where it is possible to notice the noise due to numerical reasons in inverting matrix A. In conclusion we can affirm that the method works and gave very good results.

Is important to highlight the high efficiency in terms of time reduction and memory used during the computation. In the following tables are summarized the number of nodes and the respective computational time for each application relative to FEM and WFEM.

Structure	Finite Element method	
	number of DOFs	computational time
1D beam	6603	49.31 <i>s</i>
2D beam	26422	573.30 <i>s</i>
Bridge	329004	204 <i>min</i>

Structure	Wave Finite Element method	
	number of DOFs	computational time
1D beam	33	5.57 <i>s</i>
2D beam	242	9.63 <i>s</i>
Bridge	1368	100 <i>min</i>

# Conclusions

To sum up, starting from basic concepts such as the propagation constants and the wave number, that allows to describe the propagation of waves through periodic structures, it has been possible to introduce the Wave Finite Element (WFE) method that represents the foundations of the entire report. After having rigorously exposed all the fundamental steps of the method, starting from the dynamic equation of a single period up to the wave analysis thanks to which the wave base was calculated, two different approaches for a periodic structure has been exposed: the DSM approach and the WA approach. Using this last approach, the limits for which the boundary conditions can be applied only to the boundaries of the periodic structure were underlined. We, therefore, set ourselves the goal of extending the approach to structures that are constrained in a very general way and therefore being able to admit the presence of intermediate constraints.

The basic idea was to formulate the problem so that it could be implemented on a calculation code. Thanks to the  $\mathbf{L}_s$  matrix it has been possible to succeed in our intent. Finally, through practical applications, we have validated the method by finding results that coincide with the FEM but with the advantages of obtaining a computational time that in the worst case is halved. We can, therefore, consider ourselves satisfied with the effectiveness and success of our work, considering it as a starting point for writing a future WFEM-based calculation software. The thesis presents original work for the WFE method and for this reason, a publication has been extracted which abstract has been submitted to the EMI International conference that will take place in Lyon (July 3-5 2019).

# Annex A

The equation of dynamic equilibrium in the time domain is given by

$$\mathbf{M}\ddot{\mathbf{q}}(t) + \mathbf{C}\dot{\mathbf{q}}(t) + \mathbf{K}\mathbf{q}(t) = \mathbf{f}(t) \quad (4.1)$$

The Fourier Transform of the perturbation  $\mathbf{f}(t)$  is given by:

$$\mathbf{F}(\omega) = \frac{1}{\sqrt{2\pi}} \int_{-\infty}^{\infty} \mathbf{f}(t)e^{-i\omega t} dt \quad (4.2)$$

Replacing equation (4.1) in equation (4.2) we have:

$$\mathbf{F}(\omega) = \frac{1}{\sqrt{2\pi}} \int_{-\infty}^{\infty} [\mathbf{M}\ddot{\mathbf{q}}(t) + \mathbf{C}\dot{\mathbf{q}}(t) + \mathbf{K}\mathbf{q}(t)]e^{-i\omega t} dt$$

Developing the expression:

$$\mathbf{F}(\omega) = \mathbf{M} \left( \frac{1}{\sqrt{2\pi}} \int_{-\infty}^{\infty} \ddot{\mathbf{q}}(t)e^{-i\omega t} dt \right) + \mathbf{C} \left( \frac{1}{\sqrt{2\pi}} \int_{-\infty}^{\infty} \dot{\mathbf{q}}(t)e^{-i\omega t} dt \right) + \mathbf{K} \left( \frac{1}{\sqrt{2\pi}} \int_{-\infty}^{\infty} \mathbf{q}(t)e^{-i\omega t} dt \right)$$

Where the expression in parenthesis represent the Fourier transform of  $\ddot{\mathbf{q}}(t)$ ,  $\dot{\mathbf{q}}(t)$  and  $\mathbf{q}(t)$  respectively. The Fourier Transform of:

$$\frac{d^n f(t)}{dt^n} \quad (4.3)$$

is:

$$(i\omega)^n \hat{f}(\omega) \quad (4.4)$$

Applying this property we obtain:

$$\begin{aligned} \frac{1}{\sqrt{2\pi}} \int_{-\infty}^{\infty} \ddot{\mathbf{q}}(t)e^{-i\omega t} dt &= -\omega^2 \hat{\mathbf{q}}(\omega) \\ \frac{1}{\sqrt{2\pi}} \int_{-\infty}^{\infty} \dot{\mathbf{q}}(t)e^{-i\omega t} dt &= i\omega \hat{\mathbf{q}}(\omega) \\ \frac{1}{\sqrt{2\pi}} \int_{-\infty}^{\infty} \mathbf{q}(t)e^{-i\omega t} dt &= \hat{\mathbf{q}}(\omega) \end{aligned}$$

Finally

$$\mathbf{F}(\omega) = -\omega^2 \mathbf{M}\hat{\mathbf{q}}(\omega) + i\omega \mathbf{C}\hat{\mathbf{q}}(\omega) + \mathbf{K}\hat{\mathbf{q}}(\omega)$$

# Annex B

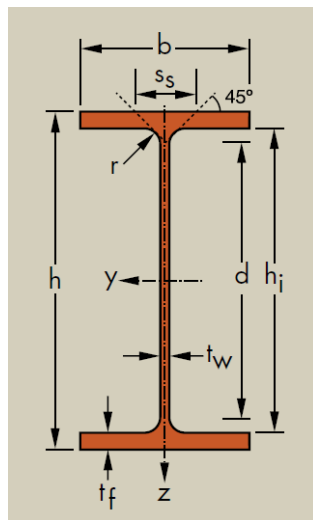


Figure 4.13: IPE 400

IPE 400	
$h$	400 mm
$b$	180 mm
$t_w$	8.6 mm
$t_f$	$\nu = 13.5$ mm

Table 4.7: Dimensions of IPE 400 section

# Bibliography

- [1] D. Duhamel, B.R. Maceb, M.J. Brennanb. *Finite element analysis of the vibrations of waveguides and periodic structures*, 2006. ISMA 2016, Sep 2016, Leuven, Belgium.
- [2] Tien Hoang, Denis Duhamel and Gilles Foret *Wave finite element method for vibration of periodic structures subjected to external loads*, 2018.
- [3] T. Hoang, D. Duhamel, G. Foret, J.L Pochet, and F. Sabatier *Wave finite element method and moving loads for the dynamic analysis of railway tracks*, 2018.
- [4] Jean-Mathieu Mencik, Denis Duhamel. *A wave-based numerical approach for fast analysis of the dynamic response of periodic structures with local perturbations*. ISMA 2016, Sep 2016, Leuven, Belgium.
- [5] Brillouin, Leon. *Wave propagation in periodic structures: electric filters and crystal lattices*. Courier Corporation, 2003.
- [6] <https://physicsworld.com/a/sound-ideas/>
- [7] <https://en.wikipedia.org/wiki/Floquet-theory>
- [8] C.Wilcox. *Theory of Bloch waves*, J.Anal. Math. 33 (1) (1978) 146-167.
- [9] L. Junyi, D.S. Balint, *An inverse method to determine the dispersion curves of periodic structures based on wave superposition*. Journal of Sound and Vibration, Volume 350, 2015, Pages 41-72, ISSN 0022-460X,
- [10] W.X. Zhong, F.W. Williams, *On the direct solution of wave propagation for repetitive structures*. Journal of Sound and Vibration, Volume 181, Issue 3, 1995, Pages 485-501, ISSN 0022-460X.

- [11] D.J. Mead, *A general theory of harmonic wave propagation in linear periodic systems with multiple coupling*, Journal of Sound and Vibration, Volume 27, Issue 2, 1973, Pages 235-260.
- [12] D.J. Mead, *Free wave propagation in periodically supported, infinite beams*, Journal of Sound and Vibration, Volume 11, Issue 2, 1970, Pages 181-197.
- [13] D. J. Mead, *Wave propagation in continuous periodic structures: research contributions from Southampton, 1964-1995*, 1995.
- [14] Ruth M. Orris, M. Petyt, *A finite element study of harmonic wave propagation in periodic structures*, Journal of Sound and Vibration, Volume 33, Issue 2, 1974, Pages 223-236.
- [15] Jamil M. Renno, Brian R. Mace, *On the forced response of waveguides using the wave and finite element method*, Journal of Sound and Vibration, Volume 329, Issue 26, 2010, Pages 5474-5488.
- [16] G. Sen Gupta, *Natural flexural waves and the normal modes of periodically-supported beams and plates*, Journal of Sound and Vibration, Volume 13, Issue 1, 1970, Pages 89-101.
- [17] J.-M. Mencik, M.N. Ichchou, *Multi-mode propagation and diffusion in structures through finite elements*, European Journal of Mechanics - A/Solids, Volume 24, Issue 5, 2005, Pages 877-898.
- [18] L. Gry, C. Gontier, *DYNAMIC MODELLING OF RAILWAY TRACK: A PERIODIC MODEL BASED ON A GENERALIZED BEAM FORMULATION*, Journal of Sound and Vibration, Volume 199, Issue 4, 1997, Pages 531-558.